Technische Universität München
TUM School of Medicine and Health

Uncovering the resistance mechanisms to *Pdk1*-deletion in PDAC

Katarína Ondrejková

Vollständiger Abdruck der von der TUM School of Medicine and Health der Technischen Universität München zur Erlangung einer

Doktorin der Medizin (Dr. med.)

genehmigten Dissertation.

Vorsitz: Prof. Dr. Gabriele Multhoff

Prüfende der Dissertation:

1. Prof. Dr. Dieter Saur
2. Prof. Dr. Günter Schneider

Die Dissertation wurde am 22.04.2024 bei der Technischen Universität München eingereicht und durch die TUM School of Medicine and Health am 10.10.2024 angenommen.

Table of contents

List of abbreviations

4-OHT	4-Hydroxytamoxifen
AKT/*Akt*	Protein kinase B
Apc	Adenomatous polyposis coli
ATP	Adenosine triphosphate
Atxn7	Ataxin 7
Atxn7L3	Ataxin 7-like 3
bp	base pair
BSA	Bovine serum albumin
Cas 9	Caspase 9
CDK8	Cyclin-dependent kinase 8
Cdks	Cyclin-dependent kinases
Cre	Cre recombinase
CRISPR	Clustered regularly interspaced short palindromic repeats
DMEM	Dulbecco's Modified Eagle Medium
DNA	Deoxyribonucleic acid
DRS	Dual recombinase system
ENY2	Enhancer of yellow 2 homolog
Erk	Extracellular signal-regulated kinase
EtOH	Ethanol
FCS	Fetal calf serum
Flp	Flippase

GDP	Guanosine diphosphate
GEMM	Genetically engineered mouse models
GSEA	Gene set enrichment analysis
GSK-3	Glycogen synthase kinase 3
GTP	Guanosine triphosphate
KO	Knockout
KRAS/*KRAS*	Kirsten Rat Sarcoma virus
loxP	Locus of X-over P1
Med12	Mediator 12
Med13	Mediator 13
Med16	Mediator 16
mTOR	Mechanistic target of rapamycin
mTORC	Mechanistic target of rapamycin complex
NSCLC	Non-small cell lung carcinoma
PBS	Phosphate buffered saline
PDAC	Pancreatic ductal adenocarcinoma
Pdk1/*Pdk1*	Pyruvate dehydrogenase kinase 1
PI3K	Phosphoinositide 3-kinase
PIP3	Phosphatidylinositol (3,4,5) triphosphate
PTEN/*PTEN*	Phosphatase and tensin homolog
PVDF	Polyvinylidene fluoride
Ras	Rat sarcoma virus
RNA	Ribonucleic acid
SAGA	Spt-Ada-Gcn5 acetyltransferase
SDS	Sodium dodecyl sulfate
sgRNA	Single-guide RNA

TFIID	Transcription factor II D
TGF-β	Transforming growth factor beta
UPS	Ubiquitin-proteasome system
Usp22	Ubiquitin specific peptidase 22
WT	Wild type

1 Abstract

Pancreatic ductal adenocarcinoma (PDAC) represents the fourth highest rate of cancer-related deaths worldwide and is predicted to become the second within the following decade. The dire prognosis of PDAC patients is caused by the mostly absent early symptoms (and subsequent late diagnosis), early distant metastasis, and relatively inefficient systemic therapeutic strategies. To this day, surgical tumor resection represents the singular curative option. However, it can lead to severe postoperative complications and require prolonged recovery time. To improve the current prognosis of PDAC patients, the identification of therapeutic targets and the development of novel therapeutic strategies are essential.

Genetically engineered mouse models (GEMM) have drastically improved understanding of PDAC carcinogenesis. Conventional *Cre/loxP* GEMMs use a single recombination step to induce PDAC. However, they do not allow the researchers to investigate the multi-step tumorigenesis of PDAC. For this reason, the Saur research group developed a novel dual recombinase (DRS) mouse model - the DRS KPF mouse model - that combines the conventional *Cre/loxP* model with *Flp/frt* recombinase to enable genetic modeling and manipulation of sequential multistep PDAC tumorigenesis.

Kirsten Rat Sarcoma virus *(KRAS)* has been identified as a major oncogenic driver in PDAC and has become the main target for therapy development. 3-phosphoinositide-dependent protein kinase 1 (Pdk1) is its important downstream effector. The DRS KPF mouse model obtains a genotype that enables a controlled tamoxifen-mediated deletion of the *Pdk1* gene. The deletion can be induced throughout tumor development. *Pdk1* ablation led to an almost complete blockage of tumor proliferation in vivo and in vitro. However, a minor cell subpopulation showed resistance against *Pdk1*-deletion-induced growth arrest. The mechanisms responsible for the survival of these cells are yet not understood. Therefore, the first objective of this work is to use the cells isolated from the DRS KPF model to investigate mechanisms responsible for the intrinsic resistance to *Pdk1* loss.

Over the last years, a range of publications emerged suggesting that members of Spt-Ada-Gcn5 acetyltransferase- (SAGA) and Mediator transcription-regulating complexes are key players in many cancer types. SAGA and Mediator are investigated in the context of poor patient prognosis, early distant metastasis, high tumor recurrence rates, and multiple cancer drug resistance. In the original functional genome-wide, CRISPR/Cas9 knockout screen performed in the Saur research group, the knockouts of some members of SAGA and Mediator were identified to promote the growth of single-cell clones resistant to the *Pdk1* loss. Therefore, the second objective of this work is to investigate the effects of the CRISPR/Cas9 mediated inactivation of SAGA and Mediator hits on PDAC carcinogens.

2 Introduction

In the first part of this chapter pancreatic ductal adenocarcinoma is introduced. Subchapters 2.1 and 2.2. discuss the problems in diagnostics, and prognosis limiting factors as well as the major therapeutic modalities. It underlines the role of PI3K/Akt signaling in PDAC carcinogenesis and describes the respective mechanisms through which PI3K/Akt signaling regulates PDAC initiation and tumor progression.

The second part of this chapter focuses on the mechanisms responsible for the resistance to the *Pdk1* loss in PDAC. It describes the CRISPR/Cas9 knockout screen, which was used to identify these mechanisms on a genome-wide scale. Finally, it introduces the SAGA and the Mediator complex, which are a major focus of this work.

2.1 Pancreatic ductal adenocarcinoma

The diagnosis of pancreatic ductal adenocarcinoma comes with a devastating life change for most of the patients. Various factors are responsible for such a dire prognosis. A delayed diagnosis due to the lack of early and disease-specific symptoms is one of them. Many patients visit their general practicians with mild back pain or cholestasis-related symptoms. These problems lead to the imagining and subsequently, PDAC detection. At this point, many of the detected tumors are already at the locally advanced stage with limited curative therapeutic approaches.

Apart from delayed diagnosis, early onset distant metastasis, heterogenic mutation profile, and poorly understood resistance mechanisms of the PDAC carcinogenesis present further important prognosis-limiting aspects.

On the curative front, surgery in combination with systemic therapy presents the only option. Regarding systemic therapy, the most common regimes are FOLFIRINOX (fluorouracil, irinotecan, leucovorin, oxaliplatin), gemcitabine/nab-paclitaxel, nanoliposomal irinotecan/fluorouracil. Local radiation presents an option for regional disease control.

2.2 PI3K/Akt signaling pathway

A mutant *KRAS* plays a critical oncogenic driving role in PDAC carcinogenesis [1, 2]. As a GTPase, it converts GTP to GDP. Upon receiving extracellular stimuli, it binds to GTP and transmits growth signals to a variety of downstream pathways. The most common mutation location is at codon 12 of the *KRAS* oncogene, resulting in the substitution of amino acid

glycine. The most common substitutions are with aspartic acid G12D or valine G12V which is responsible for over 90% of the *KRAS* mutation in PDAC [3, 4].

One of the common interactions of mutated *KRAS* is with PI3K. PI3K activation increases levels of intracellular PIP3, which in turn activates *PDK1*, an important upstream effector of the Akt signaling pathway. Phosphorylation of Thr308 induces Pdk1 a partial activation of the Akt. A complete activation of Akt follows by phosphorylation on Ser473 induced by mTOR2 Complex [5]. Enhancement of the Akt signaling plays an important role in PDAC by directly inhibiting or inducing a variety of cellular processes responsible for cell survival, cell proliferation, or cell metabolism.

To name a few examples: firstly, Akt directly inhibits FoxO1 activity and, therefore regulates programmed cell death - apoptosis. Secondly, Akt overexpression promotes the cell cycle progression by indirect activation of Cyclin D1, therefore regulating the cell cycle [6]. Thirdly, Akt regulates cell metabolism through activation of AS160 and inhibition of GSK-3 [7, 8].

In the regulation of the PI3K/Akt pathway activity, *PTEN* plays a critical role. As a ubiquitous tumor suppressor, *PTEN* dephosphorylates the inositol ring in PIP3 resulting in its inactive PIP2 form. This reaction downregulates the Akt activity. Mutation of the *PTEN* gene and consecutive loss of this downregulation has been broadly researched in the context of PDAC carcinogenesis [9].

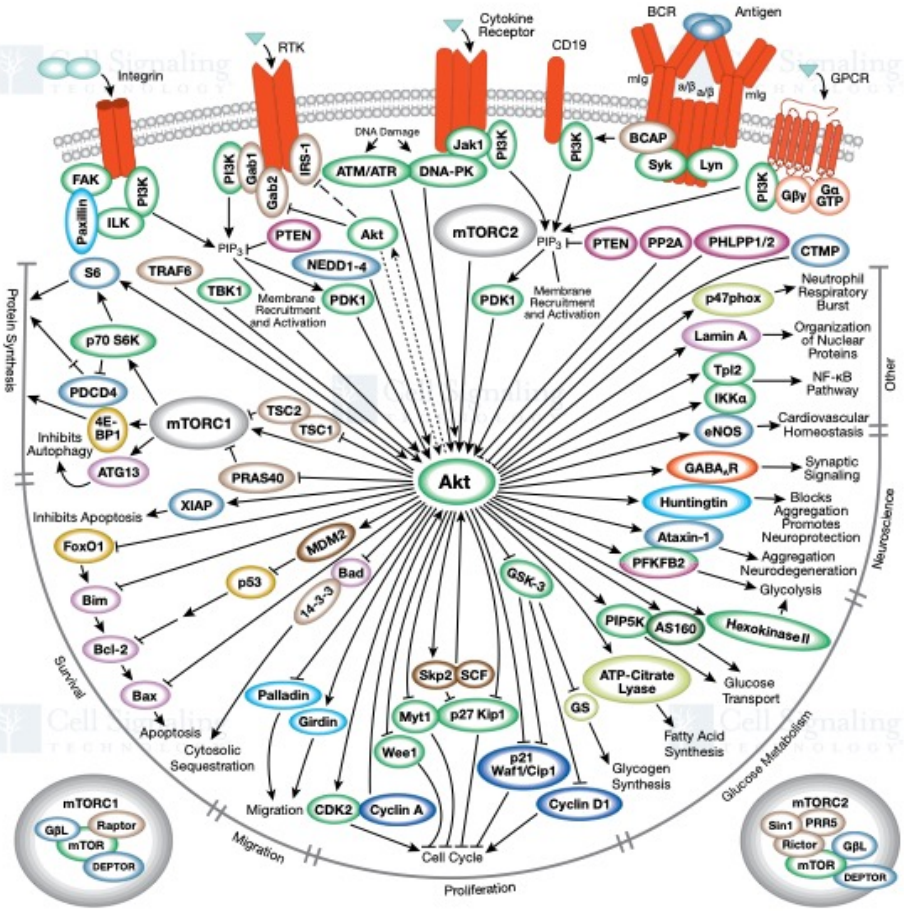

Picture 1. PI3K/Akt signaling pathway.

Courtesy of Cell Signaling Technology©

Resistance against *Pdk1*-deletion-induced growth arrest

Mutated *KRAS* being identified as the key oncogenic driver in PDAC carcinogenesis, became a main aim of research at the end of the previous century. Targeting *KRAS* directly or indirectly has shown little success in the past. To address this, the scientific focus was re-directed to one of the KRAS downstream effectors – Pdk1.

Previous work of the lab of Prof. Saur (Veltkamp, Sleiman) has shown a significant impairment of the PDAC cancer progression upon tamoxifen-mediated *Pdk1* deletion. Using cells generated from the *Pdx1-Flp; FSF- Kras$^{G12D/+}$; FSF-R26$^{CAGCreERT2/+}$; Pdk1$^{lox/lox}$* mouse model developed in Saur lab, a nearly complete PDAC tumor progression blockage in vitro and in vivo was observed. However, a minor subpopulation of the tumor cells continued proliferating independently of the *Pdk1*. Mechanisms responsible for the continuous cell proliferation, independent of *Pdk1*, remain unknown and are a focus of this work.

2.3 Genome-wide CRISPR knockout screen in PDAC

Mechanisms responsible for the resistant phenotype in PDAC carcinogenesis are yet to be identified. A novel way to do so in a singular experiment presents a pooled genome-wide CRISPR knockout screen. The manipulation of genetic information with the CRISPR system is easy and cost-efficient [10, 11]. CRISPR consists of two components – Cas9 and a single-guide RNA. As described in its name, the single-guide RNA navigates the endonuclease Cas9 to the target sequence in the gene and creates a perturbation, leading to the inactivation of the target gene. Using CRISPR in a pooled screen enables scientists to analyze numerous perturbations simultaneously [10, 11].

Such a screen was performed in the lab of Prof. Saur to identify targets responsible for *Pdk1*-resistant phenotype in the PDAC cells. Amongst the top hits of the screen, we identified members of SAGA and Mediator complexes. Screen results indicated that the lack of these complex members provides a growth advantage to the PDAC cells in the context of the *Pdk1* deletion.

2.3.1 SAGA complex

SAGA complex and transcription factor II D (TFIID) are essential coactivators regulating the transcription of protein-coding genes. SAGA complex consists of 20 subunits organized into five modules – the structural core, the TRRAP module, the metazoan splicing (SUP) module, the de-ubiquitinase (DUB) module, and the histone acetyltransferase (HAT) module [12, 13]. In this work, the focus aims at the DUB module and on the structural core as those were enriched in PDAC cells following the *Pdk1* deletion.

The DUB module of the SAGA complex consists of Ubiquitin specific peptidase 22 (Usp22), Ataxin 7 (Atxn7), Ataxin 7 L3 (Atxn7L3), and Enhancer of yellow 2 homolog (ENY2) [12–14]. The function of the DUB module is de-ubiquitination of core histones H2B and H2A by Usp22. Monoubiquitinated histone H2B on lysine 120 is associated with the enhancement of gene expression, while monoubiquitinated histone H2A with gene silencing. Therefore, Usp22 plays an important gene-regulating role. Atxn7 and ENY2 anchor the DUB module to the rest of the SAGA complex.

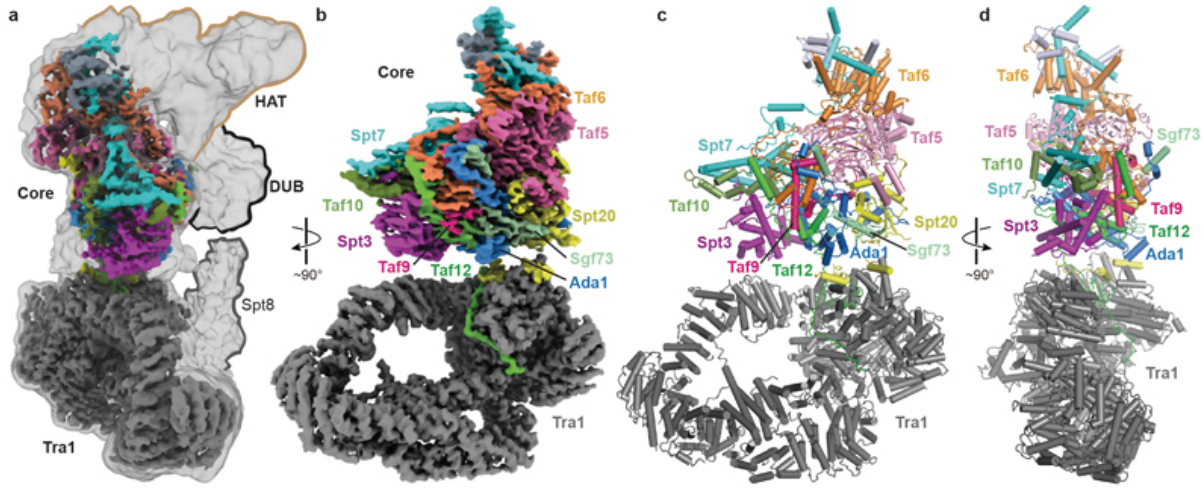

Picture 2. SAGA complex structure.

A, B. Core, HAT, Tra1, and DUB modules of SAGA complex. C, D. Structure of SAGA complex in ribbon model. Source: Structure of the transcription coactivator SAGA, Wang et al. [13]

Usp22 plays a critical role in human carcinogenesis. Marked as one of the “11-death from cancer genes” [15] its aberrant expression is associated with poor patient prognosis. It is linked to rapid tumor progression, early onset distant metastasis, and multiple cancer drug resistance [15, 16]. Despite this, more recent publications are emerging uncovering Usp22 to be depleted in many tumors with an aggressive phenotype, suggesting its role is tumor- and context-dependent [17].

Kosinsky et al. [17] describe the tumor-suppressing role of *Usp22* in an Adenomatous polyposis coli (*APC*)-mutated colorectal carcinoma via an increase in mTOR activity. Aggressive tumor growth, increased tumor volumes, and lower survival rates were observed in *Usp22*-depleted mice in comparison to the wild-type and *Usp22*-heterozygote mice. Ren et al. [9] investigated the role of de-ubiquitination by Usp22 on PTEN levels in PDAC. *PTEN* is known to inhibit the activity of the PI3K/Akt signaling pathway and thus plays an important tumor suppressive role. By silencing *Usp22* a significant PTEN degradation was observed.

2.3.2 Mediator complex

There is thriving research concerning the role of the Mediator complex in human carcinogenesis. Like SAGA, the Mediator complex also regulates the transcription by the interactions with RNA polymerase II. The Mediator complex consists of the core module (separated into head, middle, and tail) and a kinase module. The Tail Mediator connects the complex to the RNA Polymerase II [18, 19]. Two members of the mediator complex were identified in the CRISPR knockout screen and are investigated in this work – Med13 and Med16. Med13, together with Med12, CDK8, and Cyclin C, is a part of the kinase module [20]. Med16 is a connecting unit between the tail and the rest of the complex [21].

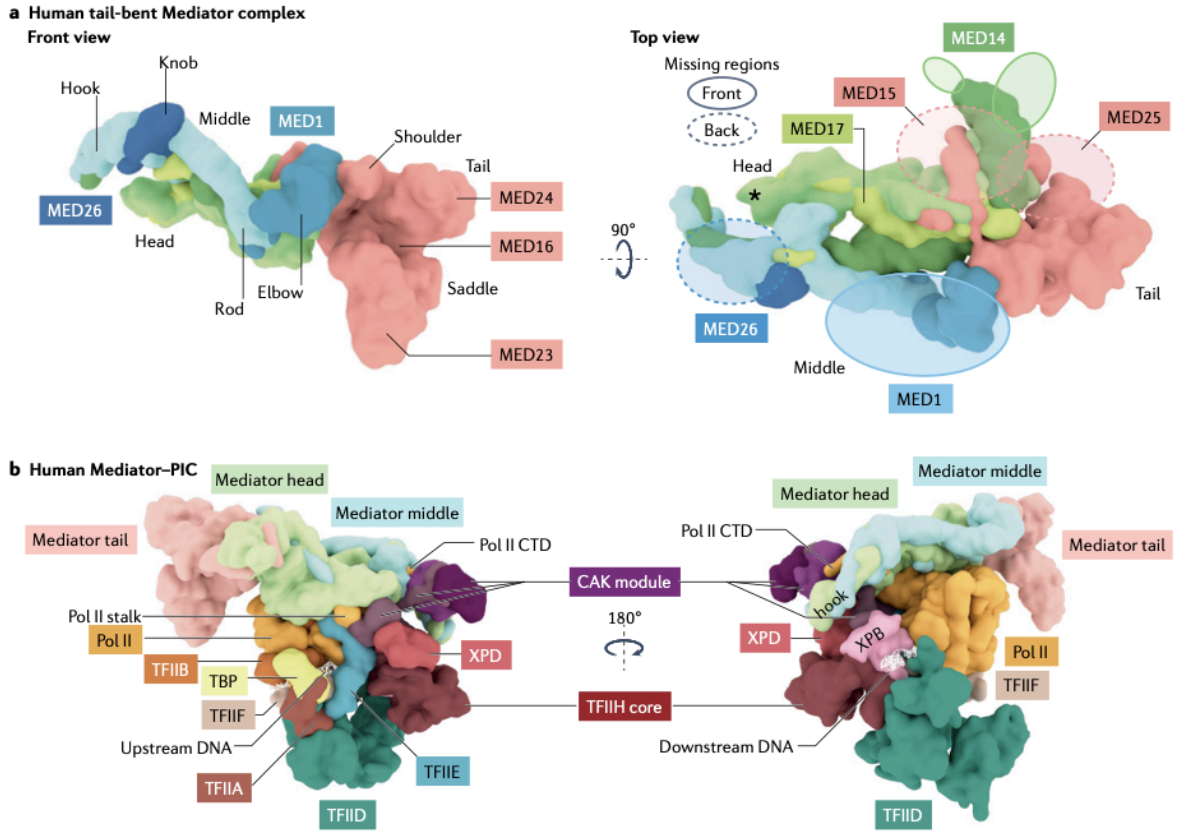

Picture 3. Structure of Mediator complex.

A. Human Mediator complex with head, core, and tail modules. B. Connection of the complex with RNA Polymerase II. Source: The Mediator complex as a master regulator of transcription by RNA polymerase II, Richter et al. [19]

The precise mechanisms through which the Mediator complex plays a role in human carcinogenesis are yet to be understood. According to recent publications interacts Med12 with the TGF-β receptor in the cytoplasm through inhibition. Low levels of Med12 in NSCLC result in an enhancement of TGF-ß signaling, which ultimately leads to epithelial-mesenchymal transition resulting in drug resistance and aggressive tumor phenotype [22].

Med16 connects the tail Mediator with the rest of the complex. There are suggestions that the depletion of Med16 and therefore a separation of the tail from the rest of the Mediator complex leads to an unspecific transcription activation. The separated tail stimulates the formation of the pre-initiation complex resulting in an enhanced transcription [21].

2.4 The aim of this work

In this work, the author aims to describe mechanisms responsible for the resistance to the *Pdk1* deletion in PDAC. The work consists of two parts – an analysis of the acute resistance and an analysis of the role of transcription complexes SAGA and Mediator in PDAC carcinogenesis. To connect the two parts, the author has researched the effects of the transcription complexes on the PDAC single-cell clones with acute resistance to the *Pdk1* loss.

To understand the acute resistance to *Pdk1* loss, I investigated single-cell clones proliferating despite the tamoxifen-induced *Pdk1* deletion. The analysis was performed on multiple levels. The RNA sequencing was performed to detect possible alterations in the transcriptome, broad western blot analysis was performed to assess the differences in PI3K/Akt signaling between resistant and sensitive clones.

In the second part of the project, I used the data of the initial genome-wide CRISPR knockout screen as an input. After throughout analysis of the top hits of the screen, we identified members of the SAGA and Mediator complexes. Upon the CRISPR-mediated knockout of these genes, we observed a significant growth advantage in the bulk cell line and the resistant clones. In this work, I performed a validation of these results. I used RNA sequencing to determine the differentially expressed genes between the knockouts and the controls and analyzed the alterations on the protein level.

To connect both parts of the project, I selected clones with the strongest resistant phenotype to the *Pdk1* deletion and with a complete growth blockage. I generated CRISPR knockouts in those clones and analyzed the effect of the knockouts as described in a previous paragraph.

This work aims to identify possible mechanisms due to which PDAC shows a poor response to systemic cancer therapy. Knowledge obtained in this project can be used to better understand the mutation profile of PDAC and to develop targeted therapies based on the mutation profile and therefore improve the dire prognosis of this disease.

3 Materials

This chapter lists the materials used to create data for this project. It is divided into seven subchapters – 3.1 Disposables, 3.2 Technical equipment, 3.3 Reagents and enzymes, 3.4 Antibodies, 3.5 Molecular biology, 3.6 Cell culture, and 3.7 Software. Chapter 3.5 is further divided into six further subchapters – 3.5.1 Primers, 3.5.2 Single-guide RNA, 3.5.3 Buffers, 3.5.4 Plasmids, 3.5.5 Bacterial strains, 3.5.6 Kits.

3.1 Disposables

Table 1. Disposables

Disposable	**Manufacturer**
6-Well CytoOne Plate	STARLAB International GmbH
Blotting Filter papers	Thermo Scientific™
Cell culture dishes 100 mm CELLSTAR	Greiner Bio-One International GmbH
Cell culture flask CELLSTAR 175 cm²	Greiner Bio-One International GmbH
Cell culture flask CELLSTAR 25 cm²	Greiner Bio-One International GmbH
Cell culture flask CELLSTAR 75 cm²	Greiner Bio-One International GmbH
Cell scrapers	Corning GmbH
Centrifuge tube 250 ml	Corning GmbH
Centrifuge tube CELLSTAR 15 ml	Greiner Bio-One International GmbH
Centrifuge tube CELLSTAR 50 ml	Greiner Bio-One International GmbH
Combitips advanced 10 ml	Eppendorf Vertrieb Deutschland GmbH
Combitips advanced 2,5 ml	Eppendorf Vertrieb Deutschland GmbH
Combitips advanced 5 ml	Eppendorf Vertrieb Deutschland GmbH

CryoPure tubes	SARSTEDT AG & Co. KG
Falcon 96-well Clear Microplate	Corning GmbH
Falcon Multiwell 48 well plate	Corning GmbH
Filtertip Biosphere 100 µl	SARSTEDT AG & Co. KG
Filtertip biosphere plus 1000 µl	SARSTEDT AG & Co. KG
Filtertip biosphere plus 200 µl	SARSTEDT AG & Co. KG
Filtropur S 0.45	SARSTEDT AG & Co. KG
Nitrocellulose membrane 0.45 µm	Thermo Scientific™
Pasteur pipettes	Hirschmann Laborgeräte GmbH & Co
PCR reaction tubes	Brand GmbH + Co. KG
Safe Lock Tubes 0,5 ml	Eppendorf Vertrieb Deutschland GmbH
Safe Lock Tubes 1,5 ml	Eppendorf Vertrieb Deutschland GmbH
Safe Lock Tubes 2 ml	Eppendorf Vertrieb Deutschland GmbH
Safe Seal microtube 0,5 ml	SARSTEDT AG & Co. KG
Safe Seal microtube 1,5 ml	SARSTEDT AG & Co. KG
Safe Seal microtube 2 ml	SARSTEDT AG & Co. KG
SafeSeal Tips Professional 10 µl	Biozym Scientific GmbH
Serological pipette CELLSTAR 10 ml	Greiner Bio-One International GmbH
Serological pipette CELLSTAR 25 ml	Greiner Bio-One International GmbH
Serological pipette CELLSTAR 5 ml	Greiner Bio-One International GmbH
Serological pipette CELLSTAR 50 ml	Greiner Bio-One International GmbH

3.2 Technical equipment

Table 2. Technical equipment

Device	**Manufacturer**

Airflow control safety cabinet	Schneider Electrotechnics
Autoclave VX-150	Systec GmbH & Co. KG
Autoclave VX-75	Systec GmbH & Co. KG
Biometra Compact electrophoresis chamber	Analytik Jena GmbH
Cell culture (aspiration controller)	BRAND GMBH + CO KG
Centrifuge 5415C	Eppendorf Vertrieb Deutschland GmbH
Centrifuge 5424R	Eppendorf Vertrieb Deutschland GmbH
Centrifuge 5425	Eppendorf Vertrieb Deutschland GmbH
Centrifuge 5427R	Eppendorf Vertrieb Deutschland GmbH
Centrifuge Multifuge X3FR	Thermo Scientific™
Centrifuge Rotina 380R	Andreas Hettich GmbH & Co
CLARIOstar microplate reader	BMG Labtech
Ecotron incubation shaker	INFORS HT
Electrophoresis power supply EPS 601	Amersham Biosciences
Electrophoresis power supply Power Pac 200	Bio-Rad Laboratories GmbH
Glassware, Schott Duran	Schott AG
Heraeus Function Line Incubator	Thermo Scientific™
Incubator Heracell VIOS 160i	Thermo Scientific™
Magnetic stirrer, Ikamag® RCT	KA® Werke GmbH & Co. KG
Microscope DM LB	Leica Microsystems GmbH
Mini-PROTEAN® Tetra Cell	Bio-Rad Laboratories GmbH
Multipipette Plus	Eppendorf Vertrieb Deutschland GmbH
NanoPhotometer	Implen GmbH
Odyssey® infrared imaging system	Li-Cor Biosciences
Pipettes PhysioCare	Eppendorf Vertrieb Deutschland GmbH

PowerPac 1000	Bio-Rad Laboratories GmbH
Rotamax 120 orbital shaker	Heidolph Instruments GmbH & CO. KG
Rotina 46R	Andreas Hettich GmbH & Co
Safety cabinet eco-safe Comfort Plus	ENVAIR Deutschland
Stripetor Plus	Corning GmbH
Thermocycler Biometra Tadvanced	Analytik Jena GmbH
Thermocycler Biometra Tgradient	Analytik Jena GmbH
Thermocycler Biometra TOne	Analytik Jena GmbH
Thermomixer Comfort	Eppendorf Vertrieb Deutschland GmbH
UVP Transluminator	Analytik Jena GmbH
Vortex genie 2	Scientific Industries, Inc.
Water bath 1003	GFL Gesellschaft für Labortechnik mbH

3.3 Reagents and enzymes

Table 3. Reagents

Reagent	**Manufacturer**
1,4-Dithiothreitol (DTT)	Carl Roth GmbH + Co. KG
2-Mercaptoethanol	Sigma-Aldrich Chemie GmbH
4-hydroxytamoxifen	Sigma-Aldrich Chemie GmbH
Acrylamide	Sigma-Aldrich Chemie GmbH
Agarose	Sigma-Aldrich Chemie GmbH
Ammonium persulfate	Sigma-Aldrich Chemie GmbH
Ampicillin sodium salt	Carl Roth GmbH + Co. KG
Bovine serum albumin	Sigma-Aldrich Chemie GmbH
Bradford reagent 5x	SERVA Electrophoresis GmbH

Bromphenol blue	Sigma-Aldrich Chemie GmbH
Calcium chloride	Carl Roth GmbH + Co. KG
CellTiter-Glo® Buffer	Promega Corporation
CellTiter-Glo® Substrate	Promega Corporation
Crystal violet	Sigma-Aldrich Chemie GmbH
Dimethylsulfoxide (DMSO)	Carl Roth GmbH + Co. KG
DNA extension ladder 1 kb	Invitrogen GmbH
DNA extension ladder 10 kb	Invitrogen GmbH
dNTP mix, 10mM	Fermentas GmbH
Dulbecco's modified eagle medium (DMEM)	Sigma-Aldrich Chemie GmbH
Dulbecco's phosphate buffered saline (PBS)	Sigma-Aldrich Chemie GmbH
Dulbecco's phosphate buffered saline, powder	Biochrom AG
Ethanol (100%)	Merck KGaA
Ethidium bromide	Sigma-Aldrich Chemie GmbH
Ethylenediaminetetraacetic acid (EDTA)	Invitrogen GmbH
Fetal calf serum (FCS)	Biochrom AG
Gibco™ Opti-MEM™ I Reduced Serum Medium	Thermo Scientific™
Glycerol	Sigma-Aldrich Chemie GmbH
Glycin	Sigma-Aldrich Chemie GmbH
HEPES	Carl Roth GmbH + Co. KG
Isopropanol	Carl Roth GmbH + Co. KG
Kalium chloride	Carl Roth GmbH + Co. KG
Luria/Miller Agar	Carl Roth GmbH + Co. KG
Luria/Miller Medium	Carl Roth GmbH + Co. KG
Magnesium chloride	Carl Roth GmbH + Co. KG

Methanol	Merck KGaA
Natrium chloride	Carl Roth GmbH + Co. KG
Non-fat dry milk	Sigma-Aldrich Chemie GmbH
Nonyl phenoxypolyethoxylethanol (N-40)	Thermo Scientific™
PageRuler pre-stained protein ladder	Thermo Scientific™
Penicillin/Streptomycin (10000 µg/mL)	Invitrogen GmbH
Puromycin dihydrochloride	Sigma-Aldrich Chemie GmbH
REDTaq® ReadyMixTM PCR reaction mix	Sigma-Aldrich Chemie GmbH
RLT Buffer	Qiagen GmbH
SDS (Natriumdodecylsulfat)	SERVA Electrophoresis GmbH
TEMED	Carl Roth GmbH + Co. KG
TransIT®-LT1 Transfection Reagent	Mirus Bio LLC
TRIS	Carl Roth GmbH + Co. KG
Triton® X-100	Merck KGaA
TWEEN 20	Sigma-Aldrich Chemie GmbH

Table 4. Enzymes, Cofactors, Inhibitors

Reagent	**Manufacturer**
BsmBI restriction enzyme	New England Biolabs GmbH
CutSmart Buffer	New England Biolabs GmbH
EcoRI HF restriction enzyme	New England Biolabs GmbH
HotStarTaq DNA polymerase	Qiagen GmbH
MluI restriction enzyme	New England Biolabs GmbH
NEBuffer 3.1	New England Biolabs GmbH
Phosphatase inhibitor	SERVA Electrophoresis GmbH
Protease inhibitor	Roche Deutschland Holding GmbH

SapI restriction enzyme	New England Biolabs GmbH
T4 DNA Ligase	New England Biolabs GmbH
T4 DNA Ligase Buffer	New England Biolabs GmbH
Trypsin, 0.05% with 0.53 mM EDTA 4Na	Invitrogen GmbH

3.4 Antibodies

Table 5. Primary antibodies

Antibody	**Manufacturer**
Akt #9272	Cell Signaling Technology, Inc.
Ataxin 7L3 #MA3-084	Thermo Scientific™
Beta-Actin (13E5) #4970S	Cell Signaling Technology, Inc.
Cyclin B1 (V152) #4135S	Cell Signaling Technology, Inc.
Cyclin D1 #2922	Cell Signaling Technology, Inc.
FoxO1 #2880	Cell Signaling Technology, Inc.
FoxO3a #2497	Cell Signaling Technology, Inc.
GAPDH (14C10) #2118S	Cell Signaling Technology, Inc.
Histone H2B (D2H6) #12364S	Cell Signaling Technology, Inc.
Hsp90 alpha/beta (F8) #SC-13119	Santa Cruz Biotechnology, Inc.
Med13 #PA5-79654	Thermo Scientific™
Pdk1 #3062	Cell Signaling Technology, Inc.
Phospho-Akt (S473) #9271	Cell Signaling Technology, Inc.
Phospho-FoxO1 (T24)/ FoxO3a (T32) #9464	Cell Signaling Technology, Inc.
Phospho-mTOR (Ser2481) #2974	Cell Signaling Technology, Inc.
Phospho-p70 S6 Kinase (Thr421/Ser424) #9204	Cell Signaling Technology, Inc.
Phospho-Pdk1 (S241) #3061	Cell Signaling Technology, Inc.

Phospho-Rictor (Thr1135) #3806T	Cell Signaling Technology, Inc.
Phospho-S6 Ribosomal Protein (S235/236) #4858	Cell Signaling Technology, Inc.
Phospho-S6 Ribosomal Protein (S240/244) #5364	Cell Signaling Technology, Inc.
PTEN (D4.3) #9188	Cell Signaling Technology, Inc.
Rictor #2114	Cell Signaling Technology, Inc.
S6 Ribosomal Protein #2317	Cell Signaling Technology, Inc.
THRAP5 #PA5-116039	Thermo Scientific™
Tuberin/TSC2 (D93F12) XP #4308	Cell Signaling Technology, Inc.
Ubiquityl-Histone(K120) (D11) XP® #5546T	Cell Signaling Technology, Inc.
Usp22 #SC-390585	Santa Cruz Biotechnology, Inc.

Table 6. Secondary antibodies

Antibody	**Manufacturer**
Anti-Mouse IgG DyLight800 SA535521	Invitrogen GmbH
Anti-Rabbit IgG DyLight800 SA535571	Invitrogen GmbH

3.5 Molecular biology

3.5.1 Primers

All used DNA Primers were synthesized by Eurofins Genomics and diluted in distilled water to the concentration of 10 μM.

Table 7. Pdk1 recombination PCR Primers

Primer Name	**Primer Sequence (5´to 3´)**
PDK1-LP	TGTGGACAAACAGCAATGAACATACACGC
PDK1-del-UP	CTATGCTGTGTTACTTCTTGGAGCACAG
Pdk1-i4-UP2	CCCTCTAGCAAATGTTCTGTCTGGAATGTCT

Table 8. Amplification PCR Primers for CRISPR Genome Editing Evaluation

Primer Name	**Primer Sequence (5´to 3´)**
Atxn7L3_sg2_Fw1	AGGGCTTAGAGCAGTCCTTTAG
Atxn7L3_sg2_Rev1	ATTTCCTTCACCCCAGCTTCTC
Atxn7L3_sg4_Fw1	GCCAGGAGATTTGGTTGGTGA
Atxn7L3_sg4_Rev1	ACCCCATAAGACTACACCTCG
Med13_sg2_Fw1	TACTGGGCAACAAGGACAGG
Med13_sg2_Rev1	TCCTATCCTATAACCAAGCCTAGC
Med13_sg3_Fw1	GAGCAGCGCACCTCCTAGTAAT
Med13_sg3_Rev1	ATGAACTGACGCCCATGTTCTA
Med16_sg3_Fw1	GAGGAAACGCCAATGCTTGT
Med16_sg3_Rev1	AGATACTCCCTGAGCCACCA
Med16_sg4_Fw1	ACATCCTCAGACCAAGTGGC
Med16_sg4_Rev1	GGCACACAGAAGCAACCCTA
Tada1_ sg1_Fw1	ACATGCGTGGTGTTCTCTGC
Tada1_ sg1_Rev1	GCCTGTCAGATAAGGTCGGTA
Tada1_ sg4_Fw1	TTGTCTCTTCCGGTTGTTACCAT
Tada1_ sg4_Rev1	ACCAACCTCCACGGCATAGA
Taf5l_sg1_Fw1	GAATGAATAGTGGCTGCCCCC
Taf5l_sg1_Rev1	GCTAAAGGCCAGACTGGTGAT
Taf5l_sg3_Fw2	CGCTTCCATGGGATGTTCCT
Taf5l_sg3_Rev2	GCTGAGTGTTGTTGGGGAGA
Usp22_sg1_Fw1	TCCGGCGCTCGTGAATTT
Usp22_sg1_Rev1	GCTATCCATTCTCCCGAGGAC
Usp22_sg2_Fw2	GCATGGTTGCTTCCAAGGAGTC
Usp22_sg2_Rev2	TAAGGTGGTGCTGAGCTTTAGG

3.5.2 Single-guide RNA Oligonucleotides

Table 9. Single-guide RNA Oligonucleotides

Oligonucleotide ID	Oligonucleotide Sequence
Atxn7l3 sgRNA2 FW_BRIE	CACCGTGTCCAAAGATGTCCAACCC
Atxn7l3 sgRNA2 Rev_BRIE	AAACGGGTTGGACATCTTTGGACAC
Atxn7l3 sgRNA4 FW_BRIE	CACCGTACACCGGGCTGTTAAGTG
Atxn7l3 sgRNA4 Rev_BRIE	AAACCACTTAACAGCCCGGTGTAC
Med13 sgRNA2 FW_BRIE	CACCGCTGTACCAACATACACGGT
Med13 sgRNA2 Rev_BRIE	AAACACCGTGTATGTTGGTACAGC
Med13 sgRNA3 FW_BRIE	CACCGATAGGACGTAACACAGACTG
Med13 sgRNA3 Rev_BRIE	AAACCAGTCTGTGTTACGTCCTATC
Med16 sgRNA3 FW_BRIE	CACCGGTGCAGCGCATAAACAGTG
Med16 sgRNA3 Rev_BRIE	AAACCACTGTTTATGCGCTGCACC
Med16 sgRNA4 FW_BRIE	CACCGCCTGGACCGTGTATCCGCGG
Med16 sgRNA4 Rev_BRIE	AAACCCGCGGATACACGGTCCAGGC
Tada1 sgRNA1 FW_BRIE	CACCGTTTCCTTCTCGACACAACTG
Tada1 sgRNA1 Rev_BRIE	AAACCAGTTGTGTCGAGAAGGAAAC
Tada1 sgRNA4 FW_BRIE	CACCGTGAGGCTGGAACCTATGCTA
Tada1 sgRNA4 Rev_BRIE	AAACTAGCATAGGTTCCAGCCTCAC
Taf5l sgRNA1 FW_BRIE	CACCGACAGAGATGAAGATTCTGCG
Taf5l sgRNA1 Rev_BRIE	AAACCGCAGAATCTTCATCTCTGTC
Taf5l sgRNA3 FW_BRIE	CACCGACTACCAGCTGTACGCCAG
Taf5l sgRNA3 Rev_BRIE	AAACCTGGCGTACAGCTGGTAGTC
Usp22 sgRNA1 FW_BRIE	CACCGCCATCGACCTGATGTACGG
Usp22 sgRNA1 Rev_BRIE	AAACCCGTACATCAGGTCGATGGC
Usp22 sgRNA2 FW_BRIE	CACCGTTGACCAGATCTTTACGGGT

Usp22 sgRNA2 Rev_BRIE	AAACACCCGTAAAGATCTGGTCAAC

3.5.3 Buffers

Table 10. Buffers

Buffer	Components
5x KCM Buffer	500 mM KCl 150 mM CaCl2 250 mM MgCl2
IP Buffer pH7.9	50 mM HEPES 150 mM NaCl 1 mM EDTA 0.5% Nonidet P40 10% Glycerol Phosphatase inhibitor Protease inhibitor
10x Gitschier Buffer	670 mM Tris, pH 8.8 166 mM (NH4)2SO4 67 mM MgCl2
Soriano Buffer	0.5% Triton® X-100 1% 2-Mercaptoethanol 1x Gitschier's buffer 400 µg/mL Proteinase K (add prior to use)
Stacking gel buffer	Tris-HCl 0.5 M, pH 6.8
Separating gel buffer	Tris-HCl 1.5 M, pH 8.8
Running buffer (10x)	35 mM SDS 250 mM Tris 1.92 M Glycine
Transfer buffer (10x) pH8.3	250mM Tris 1.92 M Glycine
Washing Buffer	PBS 0.1% Tween
5x Laemmli Buffer, pH 6.8	10% SDS 50% Glycerol

	228 mM Tris hydrochloride 0.75 nM Bromphenol blue 5% 2-Mercaptoethanol

3.5.4 Plasmids

Table 11. Plasmids

Plasmid	Source	RRID
LentiCRISPRv2	Addgene	Addgene_98290
pMD2.G	Addgene	Addgene_12259
psPAX2	Addgene	Addgene_12259

3.5.5 Bacterial strains

Table 12. Bacterial strains

Bacterial Strain	Source
RecA defficient E.coli	Endura

3.5.6 Kits

Table 13. Molecular biology kits

Kit	Manufacturer
Monarch PCR and DNA Cleanup Kit	New England Biolabs GmbH
Plasmid DNA Cleanup Kit mini	MACHEREY-NAGEL GmbH & Co. KG
NucleoBond Xtra Midi	MACHEREY-NAGEL GmbH & Co. KG
RNA, DNA, Plasmid Cleanup Kit	MACHEREY-NAGEL GmbH & Co. KG
Rneasy Micro Kit	Qiagen GmbH
QIAshredder	Qiagen GmbH
GenElute™ Mammalian Genomic DNA Prep Kit	Sigma Aldrich

3.6 Cell culture

Table 14. Cell lines

Cell Lines	Generated by
CV7250_PPT epithelial, KRAS_driven, PKPΔDEL_HET	Cristian Veltkamp/Katia Sleiman

Table 15. Cell culture media

Medium	Components
Cancer cell medium	DMEM 10% FCS 1% Penicillin/Streptomycin
Freezing Medium	70% DMEM 20% FCS 10% DMSO

3.7 Software

Table 16. Software

Software	Source
AxioVision 4.8	Carl Zeiss AG
Excel	Microsoft Corporation
GraphPad Prism 7	GraphPad Software, Inc.
GSEA V4.2.3	Broad Institute, Inc.
Odyssey v1.2	Li-Cor Biosciences
PowerPoint	Microsoft Corporation
Serial Cloner V2.6	Serial Basics
SnapGene V6.0.6.	GSL Biotech LLC
Word	Microsoft Corporation

4 Methods

This chapter describes the methods used in the experiments used to generate data for this work. It contains six subchapters – 4.1 Mouse model, 4.2 Cell culture experiments, 4.3 Molecular biology, 4.4 Protein biochemistry, 4.5 CRISPR/Cas9 mediated gene knockouts, and 4.6 Statistics and reproducibility. Picture 4 depicts a schematic overview of this chapter structure.

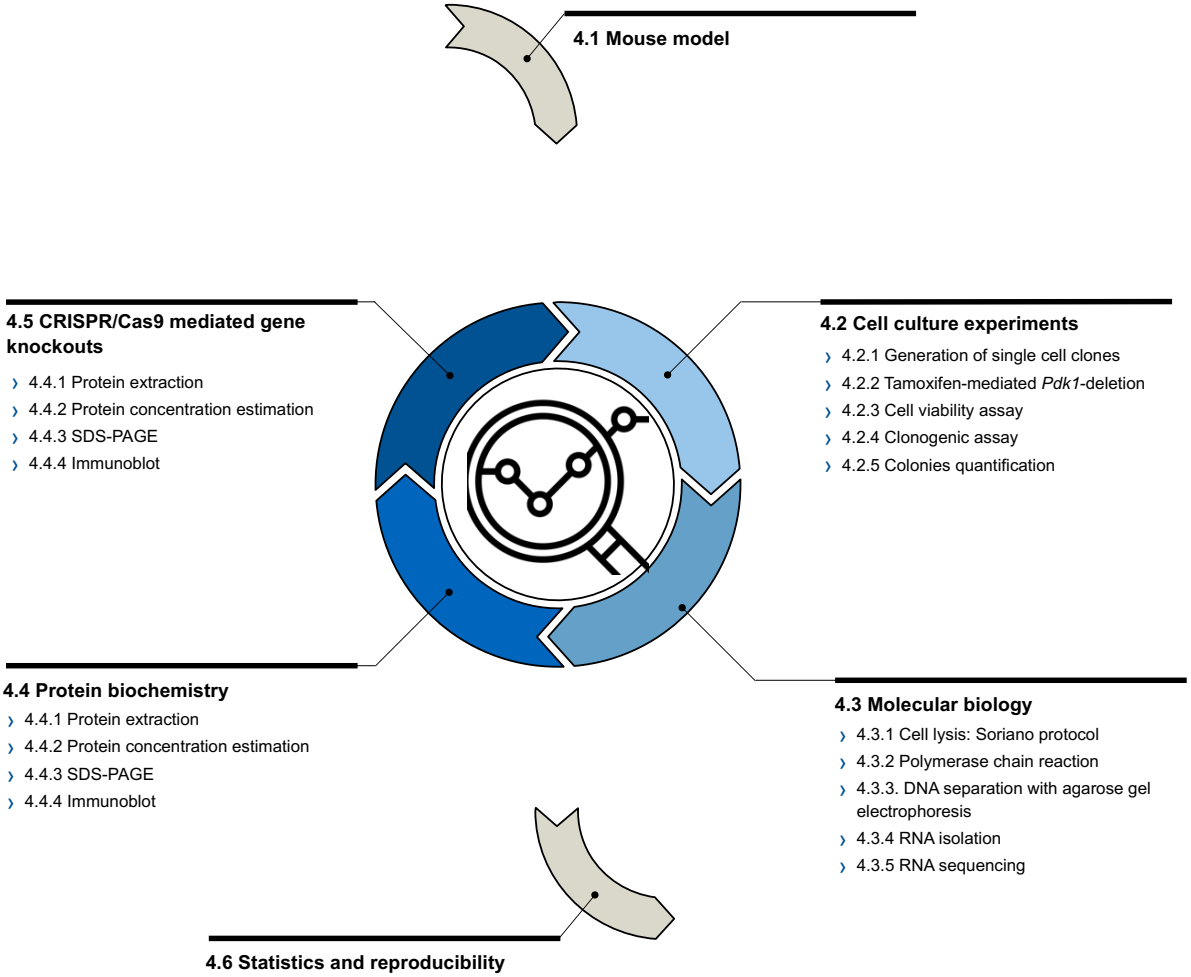

Picture 4. Methods.

The six subchapters of Chapter Methods with their sub-points.

This work used the methodical standards followed in the research group of Prof. Saur. Therefore, the following chapters can resemble the previous publications of Prof. Saur's research group members. This work follows the data obtained in the PhD thesis of Christian Veltkmap and the PhD thesis of Katia Sleiman. Veltkamp characterized the Dual recombinase mouse model with the floxed *Pdk1* allele and established the PCRs and some of the other methods. (https://mediatum.ub.tum.de/1308250). Sleiman established protocols for CRISPR/Cas9-related experiments (https://mediatum.ub.tum.de/?id=1687438).

4.1 Mouse model

This work used conditional mouse models with Cre/loxP and Flp/frt recombinase systems. Mice with flanked transgenes by *loxP* or *frt* sites were bred with mice expressing Cre or Flp recombinase. Conditional inactivation of the flanked genes was allowed by a pancreas-specific promoter. An inducible dual-recombination Flp/frt;Cre^{ERT2}/loxP system developed in the group of Prof. Saur was used to induce the time-specific inactivation of the genes [1]. All mouse strains were generated, used, and described in the PhD theses of C. Veltkamp as well as K. Sleiman as indicated above.

4.2 Cell culture experiments

All cell culture experiments were conducted on cells of the CV7250 epithelial cell line (3.6). CRISPR/Cas9 knockouts were generated using CV7250 bulk cells, one *Pdk1*-deletion resistant, and one sensitive clone (Chapter 4.2.1).

4.2.1 Generation of single-cell PDAC clones

Cryotubes containing cells of the CV7250 cell line, 4^{th} passage, were thawed in a waterbed at 37 °C, transferred into a cancer cell medium (contents listed in 3.6), and centrifuged for 5 minutes at 21°C, 1000 rpm speed. The supernatant was aspirated, and cells were re-suspended in a fresh cancer cell medium. Afterward, the cells were seeded into two 75 cm^2 cell culture flasks and incubated in an incubator at 37 °C with 5% CO_2 and 100% humidity until they reached 70 to 80% confluency.

For establishing single-cell clones, the medium was aspirated, cells were washed with 10 ml PBS and detached using 1 ml of trypsin. After the detachment was complete, a fresh cancer cell medium was added to neutralize trypsinization. Cell suspensions were diluted to a density of 0,8 cells/200µl of medium and seeded into six 96-well cell culture plates. The plates were incubated at 37 °C. The medium was exchanged in intervals of 3 days. The total incubation time of the plates was between 2 to 4 weeks depending on the growth speed of the individual single-cell clones.

During the incubation, plates were microscopically monitored to identify colony formations. Those wells were marked and numbered for identification. The numbering of the wells corresponds with the numbering of the clones. Wells containing more than one colony were crossed out of the experiment as the original inhabitation with more than one cell could not be excluded.

Clonal cultures were gradually expanded into 6-well plates. To achieve the expansion, the medium was aspirated, cells were washed with PBS and detached from the wells using trypsin.

At this point, cryopreservation of the clones was conducted. Cells were centrifuged for 5 minutes at 21 °C at 1000 rpm speed. The supernatant was aspirated, and the cell pellet was dissolved in an ice-cold freezing medium and transferred into a CryoPure tube. One sample of every clone was stored at -80 °C and later in liquid nitrogen for future use. All clones were then treated with 4-OHT to initiate *Pdk1* deletion.

4.2.2 Tamoxifen-mediated *Pdk1* deletion

To initiate the *Pdk1* deletion, CV7250 bulk cells or CV7250 single-cell clones were seeded in cell culture dishes at a density of 1 million cells/dish. 600 nM 4-OHT or EtOH was applied every 48 hours for 7 days in total. Subsequently, *Pdk1*-depleted cells were used for further experiments as described in the following chapters.

Tamoxifen-mediated *Pdk1* deletion was conducted also in the single-cell clones. To determine if the specific clone is resistant to the *Pdk1*-deletion or sensitive the proliferation of the clone after the 4-OHT treatment was observed.

4.2.3 Cell viability assay

To determine the viability of the single-cell clones independent of the Pdk1, luciferase viability assays were performed. Metabolically active, and therefore viable cells use adenosine triphosphate (ATP) to transfer energy [23]. Using a CellTiter-Glo® reagent, the cells were lysed and a luminescent signal directly proportional to the amount of ATP present was measured [23]

.4-OHT- and EtOH-treated cells were detached from the cell culture dishes using trypsin. To estimate the optimal seeding density and to prevent cell death due to overgrowing, cell suspensions were seeded in 5 opaque-walled 96-well plates at 500, 1000, and 2000 cell/well density in 4 replicas in the first experiment. Plates were incubated for 1 to 5 nights. Subsequently, the plates were equilibrated for 30 minutes at room temperature. 25 µl of CellTiterGlo® reagent was added to the wells. To induce the lysis, contents were mixed for 10 minutes on an orbital shaker. The luminescence was measured using a CLARIOstar microplate reader. The measurement was repeated on 4 consecutive days.

In the following experiments, a density of 500 cells/well was used, as here the EtOH controls have not reached the confluency before day 4. Raw luminescence values of days 1-4 were normalized to the values detected on day 0.

4.2.4 Clonogenic assay

4-OHT- and EtOH-treated cells were seeded at 2000 cells/well density in 6-well cell culture plates in 3 replicas. Plates were incubated for 10 days. The EtOH controls were at 80 to 90% confluency at that time point. The 4-OHT treated cells were seeded at 2000 cells/well density in additional 6-well plates and incubated for 15 days, to assess the late-onset proliferation effect.

After the respective incubation periods, the medium was aspirated, cells were washed with PBS and stained with 0,2% crystal violet solution. Plates were incubated overnight at room temperature on an orbital shaker. On the following day, the crystal violet solution was discarded, and plates were washed twice with distilled water and air-dried.

The photographic documentation of the grown colonies was performed on an EPSON scanner. After this, the colonies were quantified as described in the following chapter.

PDAC colonies stained with crystal violet were dissolved in 1% SDS and incubated on an orbital shaker for 4 days. Subsequently, the absorbances of the solution in the plates were measured on a CLARIOstar microplate reader.

4.3 Molecular biology

Experiments described in this chapter were conducted on cells with 4-OHT-induced *Pdk1* deletion and EtOH-treated controls generated in the cell culture experiments (4.2.1 and 4.2.2).

4.3.1 Cell lysis with Soriano protocol

Cell pellets were dissolved in 50,25 μl of Soriano final solution (contents listed in Table 17). The cell lysis was achieved on a thermocycler for 90 minutes at 55 °C, followed by 15 minutes at 95 °C. Lysed cells were vortexed for 10 seconds and centrifuged for 15 minutes at 4 °C, 14000 rpm speed. 40 μl of the supernatant containing cellular DNA was used for recombination PCR or stored at -20 °C for further use.

Table 17. Soriano final solution

Reagent	**Volume per sample**
Soriano Buffer	49 µl
Proteinase K	1 µl
DTT	0,25 µl

4.3.2 Polymerase chain reaction

To determine the Pdk1 recombination efficiency, recombination PCRs [24] were performed using a PCR pre-mix containing dNTPs, TAC polymerase, and S buffer (Table 18). PCR conditions and primer volumes are listed in Table 19.

Table 18. PCR pre-mix

Solution	**Volume for one PCR**
Distilled H2O	4,375 µl
S Buffer 10x	2,500 µl

30 % sucrose	2,500 µl
Suc Rot	2,500 µl
PeqTaq	0,125 µl
dNTPs (10 µM each)	0,500 µl

Table 19. Pdk1 recombination PCR volumes and conditions

Volume for one PCR		**Conditions**		
12,5 µl	Ready Mix	95 °C	3 min	
0,4 µl	Pdk1-i4-UP2 Primer	95 °C	45 sec	40 cycles
1,0 µl	Pdk del UP Primer	63 °C	1 min	
0,6 µl	Pdk LP Primer	72 °C	1 min 30 sec	
9,5 µl	distilled H2O	4 °C	hold	
1,0 µl	DNA			

4.3.3 DNA separation with agarose gel electrophoresis

1% agarose gel was used to separate the nucleic acids obtained as described in the previous two chapters. Agarose was dissolved in 400 ml of 1x TAE Buffer and microwaved for 6 minutes. 24 µl of Ethidium bromide was added to the mixture. DNA samples were pipetted into the prepared agarose gel pockets and ran under 115 V. The recording of the separated nucleic acids was performed using UV light (system UVP UV solo touch).

4.3.4 RNA Isolation

PDAC cells were seeded in cell culture dishes with 10 cm diameter at 1 million cells/dish density and harvested at 70 to 80% confluency. After the aspiration of the medium, the dishes were washed with ice-cold PBS. On the ice, 600 µl of RLT buffer supplemented with 6 µl of 2-mercaptoethanol were pipetted to the plates. In the next step, cells were scraped with cell scrapers and shredded in QIAshredder® columns. RNA was isolated using RNeasy® mini kits according to the manufacturer's protocol [25]. The final concentration and purity were measured using a NanoPhotometer. Samples were stored at -80 °C.

4.3.5 RNA Sequencing

RNA was isolated as described in 4.2.5. The RNA sequencing was performed according to the protocol of Saur Lab. The bioinformatical analysis of the raw sequencing data was conducted by F. Wang (Saur Group) and K. Sleiman (Saur Group). The resulting log2fold change results

generated using the DESeq Tool were shrunk to cutoff 0,5. Log2fold values of the genes with higher or equal value as a cutoff of 0,5 were used to visualize the enriched or downregulated pathways and genes.

4.4 Protein biochemistry

4.4.1 Protein extraction

Cells were seeded with 1 million cells/dish density in cell culture dishes with 10 cm diameter and harvested at 70 to 80% confluency. The medium was discarded, and dishes were washed twice with ice-cold PBS. 70-150 µl of ice-cold IP-Buffer supplemented with Protease K, and phosphatase inhibitors were added. Cells were scraped using cell scrapers and stored at -80°C.

To assess the protein concentration, samples were thawed on ice for 30 minutes followed by centrifuging for 15 minutes at 4 °C with 14 000 rpm speed. The protein-containing supernatant was aspirated and pipetted in a fresh microcentrifuge tube.

4.4.2 Protein concentration estimation

Protein concentrations were estimated with Bradford Assay. In the first step, BSA standard samples were prepared in serial dilution. The Bradford reagent was diluted with distilled water 1:5 and 300 µl of the diluted reagent was pipetted into a 96-well plate. 1 µl of protein sample or 1 µl of BSA sample was added to the wells in 3 replicas. Plates were incubated on an orbital shaker at room temperature for 30 minutes.

The absorbances were measured at 595 nm wavelength using a CLARIOstar microplate reader. The absorbances of the BSA standard probes at known concentrations were used to generate a standard curve to estimate the concentration of the PDAC protein samples. Subsequently, protein concentrations were adjusted to the same level using IP and Laemmli Buffer and denaturized in a heat block at 95 °C for 5 Minutes. Denaturized protein samples were stored at -20 °C.

4.4.3 SDS polyacrylamide gel electrophoresis (SDS-PAGE)

To separate the proteins of interest, 10% SDS-PAGE separating gels were mixed as listed in Table 20 and left to polymerize at room temperature. Isopropanol was poured on top of the gel to keep it at a straight level. After 30 minutes isopropanol was discarded, stacking gel was prepared as listed in Table 21, and poured on the separating gel. The stacking gel was left to polymerize for 30 minutes at room temperature. Protein samples were loaded into prepared wells and run under initially 100 V voltage, followed by protein separation under 140 V voltage. At the end of the run, the proteins were separated based on their molecular weight.

Table 20. Contents of 10% separating gel

Reagent	**10% separating gel**

H2O	1500 µl
Separating gel buffer	650 µl
30% acrylamide	375 µl
10% SDS	25 µl
10% APS	12.5 µl
TEMED	5 µl

Table 21. Contents of stacking gel

Reagent	**Stacking gel**
H2O	2050 µl
Stacking gel buffer	1300 µl
30% acrylamide	1650 µl
10% SDS	25 µl
10% APS	12.5 µl
TEMED	5 µl

4.4.4 Immunoblot

After separation, the proteins were blotted on a PVDF membrane, previously activated in a transfer buffer. The transfer from the gel to the membrane was carried out using an electric chamber with 300 mA for 2 hours. To eliminate unspecific protein bands, the membranes were incubated in PBS with 0,1% TWEEN and 5% dried milk powder mix for 60 minutes at room temperature.

Primary antibodies diluted in PBS with 0,1% TWEEN and 5% dried milk powder mix according to the manufacturer's recommendations (from 1:600 to 1:1000) were applied. The primary antibodies used in this work are listed in Tables 5 and 6 (Chapter 3.4). Membranes with primary antibodies were incubated overnight at 4 °C. On the following day, the primary antibody was either discarded or collected for re-using and membrane washed thrice with PBS 0,1% TWEEN mix for 15 minutes at room temperature.

The recommended secondary antibody (rat, rabbit, or mouse) diluted 1:10000 in PBS with 0,1% TWEEN and 5% dried milk powder mix was applied. The membrane with secondary antibody was incubated for 60 minutes at room temperature, followed by re-washing thrice with PBS 0,1% TWEEN mix for 15 minutes. The imagining of proteins was performed on 700 and 800 nm wavelengths using the Odyssey infrared system.

4.5 CRISPR/Cas9-mediated gene knockouts

CRISPR/Cas 9 mediated gene knockouts were generated in target cells of the CV7250 Bulk cell line. After the top hits of the CRISPR/Cas9 knockout screen were identified in the bulk cell line, the analysis was performed anew to examine the effect of the gene knockouts on the PDAC single-cell clones. Based on the results of the experiments described in previous chapters (4.2.1 and 4.2.2), one Pdk1-deletion-resistant and one -sensitive clone were selected. Those clones were resistant clone 19 and sensitive clone 7. Subsequently, CRISPR/Cas9-mediated gene knockouts were generated in those clones.

Oligonucleotides for single-guide RNAs (sgRNAs) were generated using Brie Library from Addgene and synthesized by Eurofins Genomics.

Primers for the PCR reactions for measuring the cutting efficiency of the sgRNAs were designed using the USCS genome browser, Serial cloner, and Primer Blast web tool. The designed primers were ordered from Eurofins Genomics. Primer sequences are listed in Table 8.

Plasmid Vector LentiCRISPRv2 Puro, with Ampicillin and Puromycin resistance gene, bacterial origin of replication, and Cas9, were obtained from Addgene.

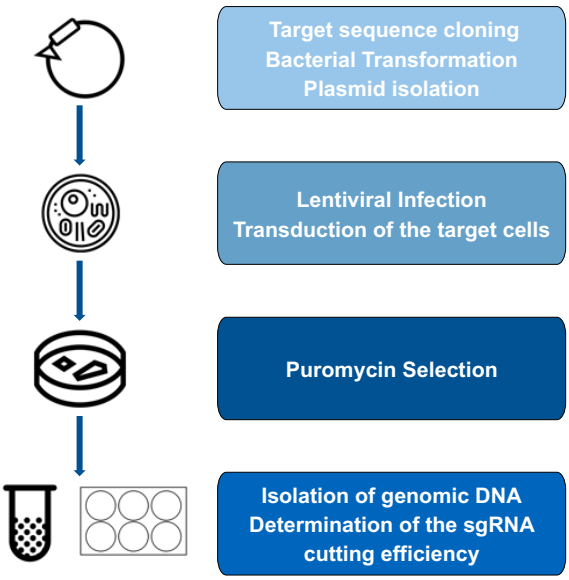

Picture 5. Generation of the CRISPR/Cas9-mediated gene knockouts.

Knockouts were performed in the CV7250 bulk PDAC cell line, Pdk1-deletion resistant Clone 19, and sensitive clone 7. Each step is described in the following subchapters. Icons are from ©Noun Project Inc.

4.5.1 Target sequence cloning

Cloning was performed according to the protocol of Zhang Lab [26]. The de-salted oligonucleotide powders were dissolved in distilled water to achieve a concentration of 100 pmol/µl. In the first step, RNA oligonucleotide annealing was performed. The reagents were pipetted as listed in Table 22 and incubated at 95 °C for 5 minutes. Afterwards, they were slowly cooled down to room temperature and diluted 1:50 in distilled water.

Table 22. Reagents and volumes for oligonucleotides annealing.

Reagent	Volume
Forward Oligo	1 µl
Reverse Oligo	1 µl
10x T4 DNA Ligase Buffer (NEB)	1 µl
ddH_2O	7 µl

In the second step, a Golden Gate assembly was performed. The LentiCRISPRv2 Puro vector was diluted to the final concentration of 90 ng/µl. The final reaction mix was pipetted as listed in Table 23. To generate DNA overhangs of the plasmid backbone and the annealed oligonucleotides, fragments were digested using the BsmBI restriction enzyme engineered by NEB. The restriction and ligation were performed in a thermocycler (Table 24). One reaction was performed without adding the oligonucleotides as a ligation control.

Table 23. Golden Gate assembly reagents and volumes.

Reagent	Volume
Annealed and diluted oligonucleotide	1 µl
LentiCRISPRv2 Plasmid at 90 ng/µl	1 µl
10x T4 DNA Ligase Buffer (NEB)	2 µl
BsmBI (NEB 10000 U/ml)	1 µl
T4 DNA Ligase (NEB)	1 µl
ddH2O	14 µl

Table 24. Thermocycling conditions.

Temperature	Time	
37 °C	5 min	10 cycles
16 °C	10 min	
55 °C	5 min	
80 °C	5 min	
10 °C	hold	

4.5.2 Bacterial transformation

For the replication of the plasmids with sgRNA sequences, a bacterial transformation was performed using recA-deficient E. coli bacteria. The reaction mixture was pipetted as listed in Table 25 and incubated for 20 minutes on ice, followed by 10 minutes of incubation at room temperature. Subsequently, 1 ml of Luria Miller medium was added. The reaction mix was then incubated for 1 hour at 37 °C at 220 rpm speed. 300 µl of the reaction mix was then plated onto Luria Miller agar plates containing ampicillin as a selection marker and incubated overnight at 37 °C.

Table 25. Bacterial transformation mixture reagents and volumes.

Reagent	Volume
Golden Gate assembly product	10 µl
5x KCM Buffer	20 µl
ddH2O	70 µl
DH10 bacteria	100 µl

4.5.3 Plasmid isolation

One day after bacterial transformation, regularly dispersed colonies grew. One colony was picked using a 10 µl pipette tip, put into 1,5 ml Luria Miller media containing ampicillin, and incubated in an orbital shaker for 5 hours at 37 °C, 220 rpm speed. After the first incubation step, the small bacteria culture was dispersed in 200 ml Luria Miller medium containing ampicillin and incubated overnight in an orbital shaker at 37 °C, 220 rpm speed. Glycerol stocks were stored for future use in -80 °C.

Subsequently, the plasmid DNA was purified from bacteria using a Macherey-Nagel Nucleo Bond Xtra Midi purification kit according to the manufacturer's protocol [27]. The final concentration and purity ratio of the plasmid DNA were measured using a NanoPhotometer and stored at 4 °C.

The purity of the plasmid DNA was confirmed with enzymatic digestion of the plasmid DNA product.

4.5.4 Lentiviral infection

Production of the lentivirus

To produce the lentivirus, human embryonic kidney 293 FT (HEK293 FT) cells were seeded in cell culture dishes with 10 cm diameter at a density of 3 million cells/dish using 10 ml of cancer cell media. On the following day, the old medium was exchanged using 9 ml of fresh cancer cell media. The transfection mix was prepared using 2 packaging plasmids – pMD2 and psPAX,

and a plasmid containing sgRNA of interest. The components of the transfection mix are listed in Table 26.

The final mix was incubated for 20 minutes at room temperature. Next, it was added dropwise to the cell culture plates containing HEK293 cells and incubated overnight at 37 °C. On the following day, the old medium was exchanged for 6 ml of the fresh medium.

Subsequently, the medium containing a high concentration of the lentivirus was collected 48 hours post-transfection. It was filtered using 0,45 μm filter and used directly for transduction of the target cells or stored in 1 ml aliquots at -80 °C for future use.

Table 26. Transfection mix.

Component	**Volumes for 1 Plate**
Opti-MEM	1500 μl
psPAX	6.3 μg
pMD2	4.1 μg
POI	8.2 μg
TransIT-LT1	55 μl

Transduction of the target cells

Target cells were seeded in 6-well plates at a density of 200-250 000 cells/well using 2 ml cancer cell media. When at 30-50 % density, the medium was exchanged for 1 ml of fresh medium containing Polybrene in 8 μg/ml concentration. 200 μl of lentivirus was added to each well. 2 wells were left uninfected as a positive and negative control. Target cells with lentivirus were spin-infected by centrifuging for 30 minutes at 33 °C, 1000 g speed, and incubated at 37 °C.

24 hours post-transduction, the old medium was aspirated, and 2 ml of fresh medium was added to the wells. 48 hours post-transduction, antibiotic selection with puromycin at a final concentration of 2,5 μg/ml was started. The medium containing puromycin was changed every 48 hours until all cells of the control sample died.

4.5.5 Isolation of genomic DNA of CRISPR/Cas 9 gene knockout

Cells were seeded at 1 million cells/dish density in cell culture dishes with 10 cm diameter and harvested at 70-80% confluency. The medium was discarded, and dishes were washed with ice-cold PBS. 800 μl of ice-cold PBS was added, and cells were scraped with a cell scraper. Cell/PBS suspensions were centrifuged for 10 minutes at 14000 rpm speed. The supernatant was discarded. Cell pellets containing up to 5 million cultured PDAC cells were used to obtain genomic DNA. The DNA purification was performed using a Sigma Aldrich Mammalian genomic DNA purification kit according to the manufacturer's protocol [28]. The final

concentration and purity of the isolated genomic DNA were determined using a NanoPhotometer and stored at -20 °C for future use.

4.5.6 Determining of the sgRNA cutting efficiency

To assess the efficiency of CRISPR/Cas9 genome editing, the DNA of the cells containing target sgRNA and control sgRNA were isolated as described in 4.5.5. PCR amplification of the regions enclosing the editing site was performed according to the Brinkman and van Steensel protocol [29]. The aliquots of the PCR products were checked on 2 % agarose gels and purified using a Monarch PCR Cleanup Kit from NEB according to the manufacturer's protocol [30]. The concentration and purity of the DNA products were measured using NanoPhotometer.

Purified PCR products of the CRISPR/Cas9 knockout cells and the controls were sent to Eurofins Genomics for Sanger sequencing [24]. The resulting sequences in a .scf format were analyzed using the TIDE Web tool (available at http://tide.nki.nl). As an input, a sgRNA sequence was added. The target sequence read within an alignment window was compared to that of a control to determine the offsets between the two sequences [29] Calculations were performed automatically by the TIDE software. The indel size range was adjusted to the maximum.

4.6 Statistics and reproducibility

All graphs were generated in GraphPad Prism 7. The mean values were normalized to the mean values of the controls (day 0 of the experiment, control sgRNA). Mean values of the luminescence in cell viability assays of the PDAC clones were normalized to day 0 of the experiment and depicted as normalized values in XY-Graphs ± standard deviation (SD).

The mean values of the absorbances of the clonogenic assay plates were normalized to the mean values of the absorbance of the controls and depicted as normalized values in bar graphs ± SD. Experiments were seeded in triplicates (n = 3) and repeated two times in the same conditions to obtain data in three technical replicates. Exception from this is the comparison between CRISPR/Cas9-mediated gene knockouts of SAGA and Mediator complex in sensitive clone 7 and resistant clone 19. This experiment was performed in a singular seeding in triplicate for every knockout.

To statistically analyze the cell culture experiments a variance was calculated followed by a two-tailed t-Test to estimate the statistical significance. $p < 0,05$ was deemed as statistically significant.

RNA Sequencing data of CRISPR knockouts and consecutively the differential gene expression analysis was by Fengchong Wang. The differentially expressed genes with an adjusted p-value of $p < 0,05$ were considered statistically significant.

5 Results

This chapter presents the main results of this work. It is divided into three main chapters (5.1, 5.2, and 5.3) as shown in Picture 6, and analyses different aspects of the resistance of PDAC to the *Pdk1*-deletion-induced growth arrest.

Chapter 5.1 analyzes the acute resistance of the *Pdk1 deletion*. By generating the single-cell clones of the epithelial PDAC cell line, it describes the differences between Pdk1-deletion-resistant and -sensitive clones. The five subchapters, 5.1.1 to 5.1.5, describe differences between those clones on multiple levels, such as transcriptome or signaling pathways.

Chapter 5.2 is based on the genome-wide CRISPR/Cas9 knockout screen conducted by K. Sleiman, marking the enrichment of the members of transcription complexes SAGA and Mediator in Pdk1 deletion-resistant clones. The validation experiments of the screen are summarized in the subchapters 5.2.1 to 5.2.3. The original genome-wide CRISPR/Cas9 knockout screen is described in detail in the PhD Thesis of K. Sleiman.

To connect the two previous parts of this work, two clones with the strongest phenotype to *Pdk1*-deletion were selected – resistant Clone 19 and sensitive Clone 7. The effect of the CRISPR/Cas9-mediated gene knockouts of the SAGA and Mediator complex is described in Chapter 5.3.

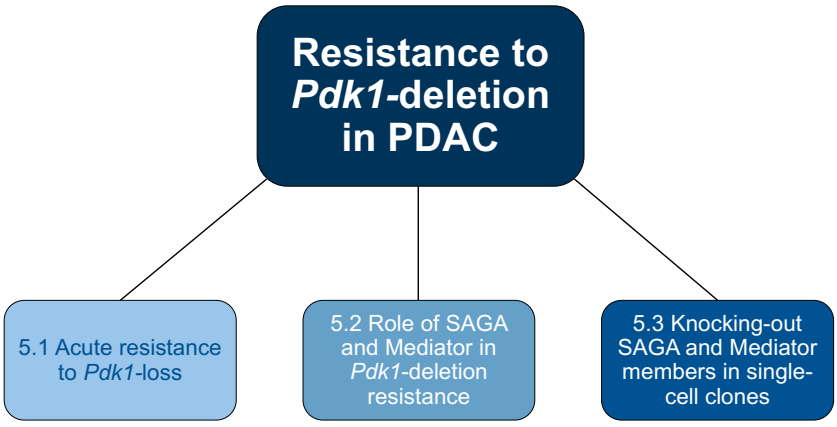

Picture 6. Results.

Structure of Chapter 5.

5.1 Acute resistance to Pdk1-loss

This chapter describes the acute resistance of PDAC cells to 4-OHT-induced Pdk1-loss. Single-cell clones were generated from a bulk cell line CV7250 at a very low passage. Subsequently, Pdk1-loss was induced by 4-OHT treatment. Clones were separated into two main comparison groups – Pdk1-deletion resistant clones continued proliferating independent of the *Pdk1*-loss; sensitive clones were arrested in their growth. The following subchapters explain the result of this work regarding the resistance.

5.1.1 One-tenth of the PDAC clones show pre-existing resistance to acute Pdk1-loss

In total, 112 single-cell clones of the PDAC CV7250 cell line were generated in the original experiment, which is described in detail in Subchapter 4.2.1. After two weeks of incubation, during which only one colony was observed, the clone was selected for expansion and 4-OHT treatment to induce *Pdk1*-deletion. Out of all selected clones, 24 continued to proliferate independently of the Pdk1, while the rest were arrested in their growth.

To confirm the categorization into resistant or sensitive groups, the primary screen was repeated in a controlled manner – seeding only 112 single-cell clones in three replicates. Out of the 24 single-cell clones previously assessed as *Pdk1*-deletion-resistant, 10 confirmed the proliferation despite the Pdk1-loss in the second experiment and were finally labeled as resistant. These clones are clone 1, 3, 6, 17, 19, 37, 66, 84, 98, and 114. In the final quantification of the PDAC single-cell clones, 92% are arrested in their proliferation in the Pdk1-depleted state, and 8% continue to grow despite the lack of the Pdk1.

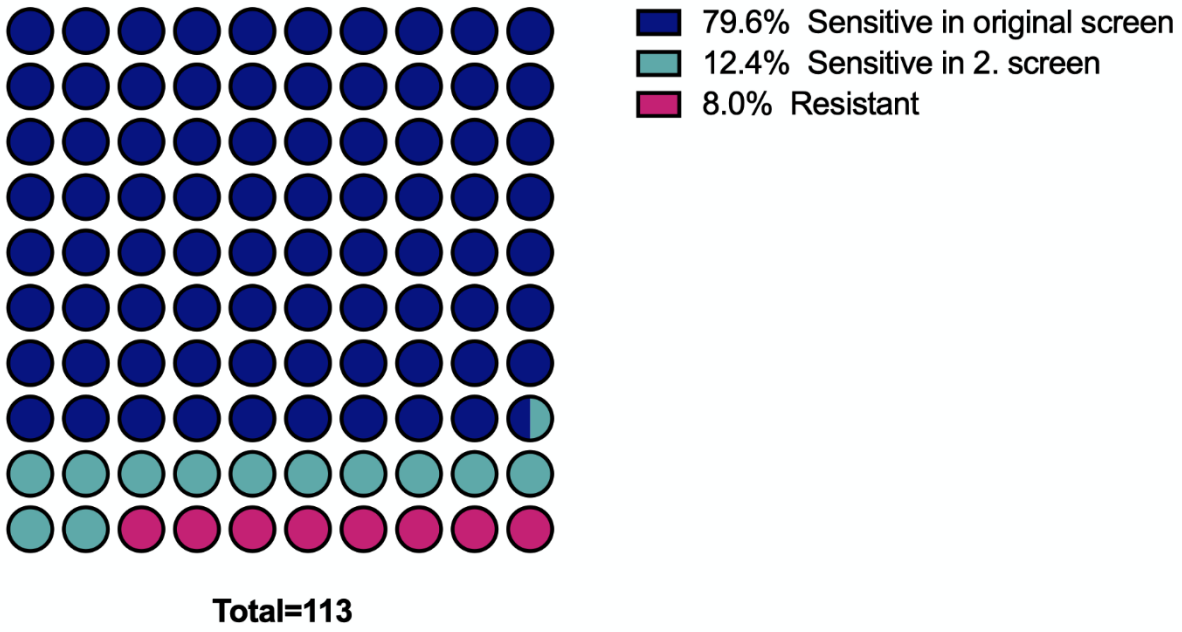

Figure 1. Quantification of the Pdk1-deletion-resistant clones.

5.1.2 Complete Pdk1 recombination in the single-cell clones was confirmed at the genomic and protein level

To exclude that the proliferation observed in the resistant clones was due to incomplete Pdk1 deletion, we assessed Pdk1 status in the clones using both recombination PCR and western blot. All the single-cell clones, including the resistant clones, generated from the PDAC CV7250 cell line showed complete recombination of the Pdk1 and therefore sufficient gene inactivation. The recombination PCR of the resistant clones is shown in Figure 2.

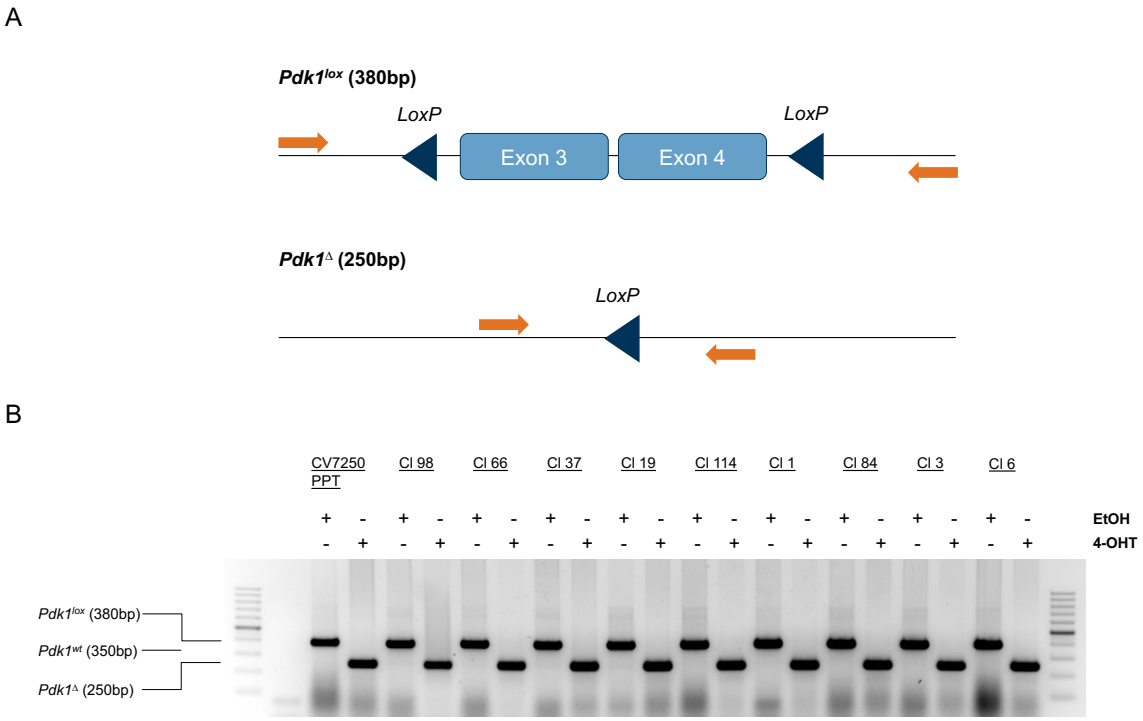

Figure 2. *Pdk1* recombination PCR of the resistant clones to assess the *Pdk1* status.

A. Schematic overview of the genotyping strategy to detect a non-recombinant and recombinant *Pdk1*. **B.** Polymerase chain reaction (PCR) of the CV7250 cell line and of the single clones to identify recombination status of the *Pdk1* upon 600 nM 4-OHT treatment as well as *Pdk1* status in the corresponding control group treated with EtOH for a total of 7 days. The upper band indicates non-recombined *Pdk1* (380bp), the band in the middle wild-type *Pdk1* (350bp), whereas the lower one (250bp) fully recombined gene.

In addition, deletion of *Pdk1* was confirmed with the western blots with no Pdk1 protein detected. Western blots of the single-cell clones were performed as described in Chapter 4.4.

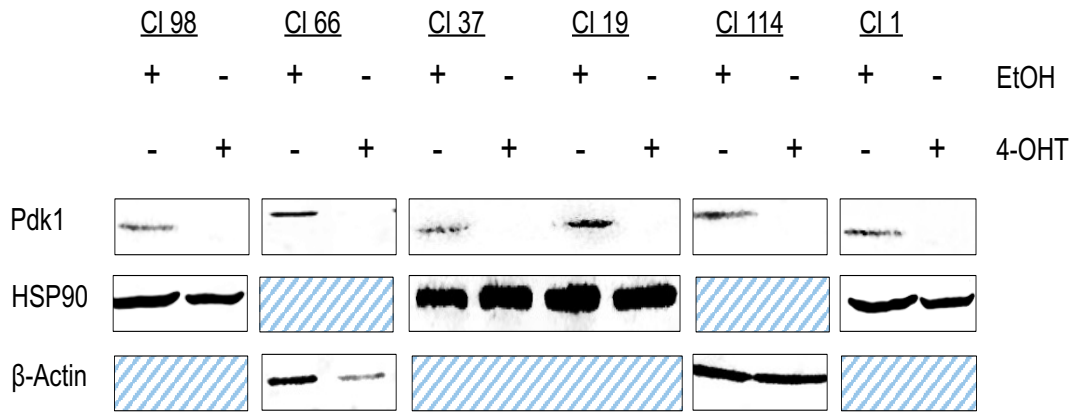

Figure 3. Western blot of the resistant clones confirmed the successful *Pdk1* deletion.

To confirm the loss of the functional *Pdk1*, western blots of the clones were performed. Figure 3 shows a schematic overview of the *Pdk1*-deletion-resistant CV7250 single-cell clones after 7 days of EtOH or 600 nM 4-OHT treatment. The first row shows Pdk1-antibody, second and third two loading controls – HSP90 and ß-Actin.

5.1.3 The late-onset proliferation of the resistant clones is Pdk1-independent

To understand how the resistant clones proliferate despite the Pdk1-loss two different experiments were performed. Cell viability analysis was performed, to evaluate whether there is a rapid proliferation in the first 4 days after the 4-OHT treatment. The assay was performed as described in Chapter 4.2.3. Some of the resistant clones showed a certain level of growth after the first 4 days, however, the general proliferation of the resistant clones was not significantly higher than the proliferation of the sensitive ones.

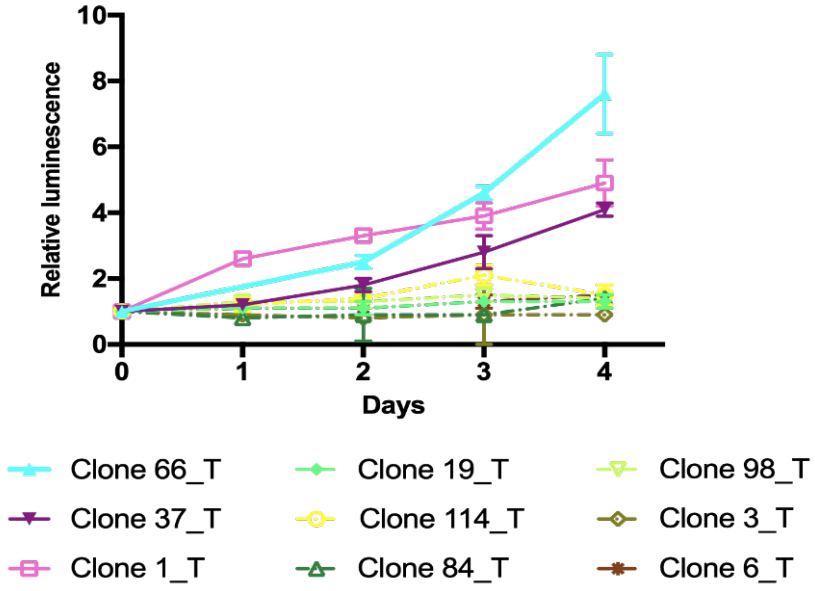

Figure 4. Cell viability assay showed no significantly elevated early-onset proliferation of the resistant clones.

500 cells/well were seeded in triplicates after 7 days of 600nM 4-OHT or EtOH treatment. The plates were incubated for 5 days in total. On each day, the luminescence of one plate was measured with values measured on day 0 (24 hours post-seeding) used as a normalization. The figure shows luminescence curves relative to day 0 of the resistant clones. Some of the clones showed proliferation on day 4, however not significantly higher than the sensitive clones. p = 0,28.

To assess the late on-set proliferation, up to 14 days after *Pdk1* deletion, a clonogenic assay was performed. In this experiment, the plates were left proliferating for up to two weeks after 4-OHT or EtOH treatment. After the incubation period plates with seeded clones were stained with crystal violet to estimate whether there was a colony formation and if so to which extent.

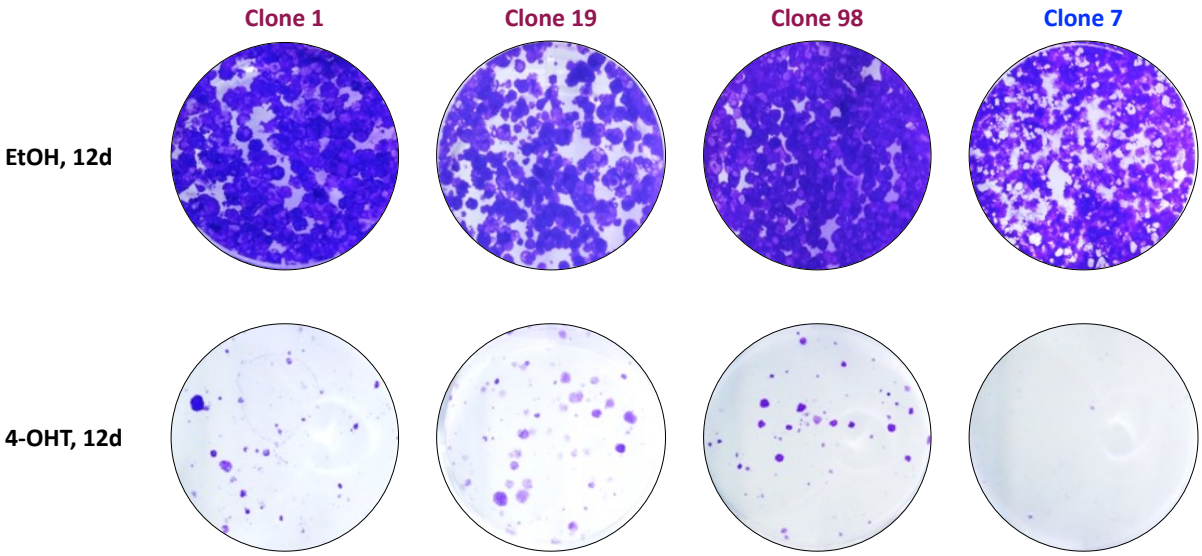

Figure 5. Clonogenic assays showed elevated proliferation of the resistant clones.

To assess the late-onset proliferation of the clones independent of the Pdk1, clonogenic assays were performed. Clones were treated with 600 nM 4-OHT or EtOH control for 7 days to induce the *Pdk1* deletion. Subsequently, they were re-seeded in fresh cancer medium and incubated for 12 days at 37°C. To visualize the proliferation, plates were washed with PBS, stained with crystal violet, and air-dried. This figure shows the results of resistant clones 1, 19, and 98, and sensitive clone 7 for comparison.

5.1.4 Differential gene expression analysis of the clones

RNA sequencing was performed to determine differentially expressed genes in resistant and sensitive clones. RNA of 7 resistant and 11 sensitive clones was harvested 7 days after 4-OHT and EtOH treatment. The bioinformatical analysis was conducted by F. Wang of the group for Prof. Saur. Significantly up- or down-regulated pathways were determined using Gene set enrichment analysis (GSEA).

The analysis highlighted a significant upregulation of proteasome in *Pdk1-deletion-resistant* clones. 26S proteasome, a part of the ubiquitin-proteasome system (UPS), is described as a

major cellular degradation system [31]. Its functions are regulation of protein-degradation as well as of the cell cycle and transcription. Therefore, there is a vast expansion in the proteasome inhibitor drugs in the context of cancer. One of the effects is the inhibition of p53 degradation and therefore boost of the tumor-suppressing effect of p53. Another is the regulation of the intracellular levels of cyclins and cyclin-dependent kinases (Cdk), which regulate the cyclin levels. The proteasome-induced degradation of Cdks and therefore overexpression of cyclins is reported in many cancer types [32].

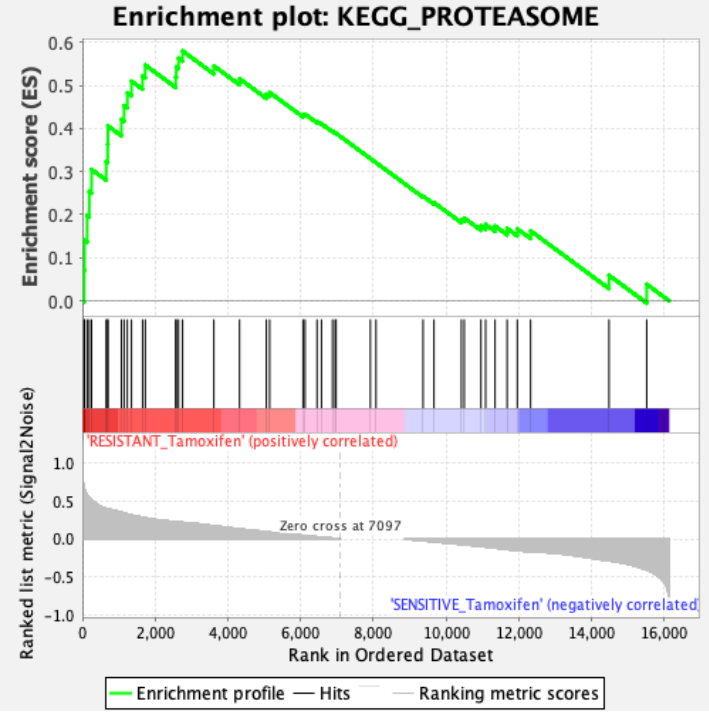

Figure 6. Proteasome pathway significantly enriched in resistant clones.

To identify differentially expressed pathways in CV7250 clones resistant to *Pdk1* deletion, RNA sequencing of the clones was performed. Bioinformatical analysis was performed by F. Wang. The main comparison of interest was Pdk1-deletion-resistant and sensitive clones. GSEA software was used to identify the hallmarks. Results show significant upregulation of proteasome, NES 1,9, p-value 0,004.

5.1.5 Role of the PI3K/Akt signaling in the resistance of PDAC clones

PI3K/Akt signaling pathway plays a major role in PDAC carcinogenesis. First, the aim was to determine whether the differences in the functions of the PI3K/Akt signaling are one of the causes of the resistance to the *Pdk1* deletion. The major pathway regulators and effectors, such as the mTORC2, family of cyclins, GSK-3, or PTEN, were analyzed closely. Western blots which were performed in a broad experiment comparing the resistant and sensitive clones are listed in Figure 7, part A. The final blots are shown in Figure 7, part B.

Importantly, to confirm the complete deletion of the *Pdk1*, *a* western blot using a Pdk1, and phosphor Pdk1 on Ser 241 was performed with the proteins from all assessed clones. No Pdk1

or phosphor Pdk1 Ser241 protein product was detected in 600 nM 4-OHT treated cells in immunoblot showing a satisfactory *Pdk1*-recombination.

A

Clone	Assesment	Pdk1	pPdk1 Ser241	pAkt Ser473	Rictor	pRictor Thr1135	p mTOR Ser2481	S6	pS6 S240/244	pS6 S235/236	pP70 S6 Thr 421/Ser424	PTEN	FoxO1	pFoxO1 Thr24	Cyclin D1
Cl 66	resistant	Pdk1	p Pdk1		Rictor	p Rictor	p mTOR	S6	p S6			PTEN			
Cl 37	resistant	Pdk1	p Pdk1	p Akt	Rictor	p Rictor	p mTOR	S6	p S6	p S6	p P70 S6	PTEN	FoxO1	p FoxO1	Cyclin D1
Cl 19	resistant	Pdk1	p Pdk1	p Akt	Rictor	p Rictor	p mTOR	S6	p S6	p S6	p P70 S6			p FoxO1	
Cl 114	resistant	Pdk1	p Pdk1	p Akt		p Rictor	p mTOR	S6	p S6	p S6	p P70 S6	PTEN	FoxO1	p FoxO1	Cyclin D1
Cl 1	resistant	Pdk1	p Pdk1		Rictor		p mTOR	S6		p S6	p P70 S6	PTEN	FoxO1	p FoxO1	Cyclin D1
Cl 84	resistant	Pdk1			Rictor			S6							
Cl 98	resistant	Pdk1	p Pdk1		Rictor		p mTOR	S6		p S6	p P70 S6	PTEN	FoxO1	p FoxO1	Cyclin D1
Cl 6	resistant	Pdk1		p Akt	Rictor			S6				PTEN	FoxO1		Cyclin D1
Cl 49	sensitive	Pdk1	p Pdk1		Rictor	p Rictor	p mTOR	S6	p S6			PTEN			
Cl 59	sensitive	Pdk1	p Pdk1		Rictor	p Rictor	p mTOR	S6	p S6			PTEN			
Cl 2	sensitive	Pdk1		pAkt	Rictor	p Rictor		S6		p S6	p P70 S6				
Cl 23	sensitive	Pdk1		p Akt	Rictor	p Rictor		S6		p S6	p P70 S6				
Cl 63	sensitive	Pdk1			Rictor			S6				PTEN	FoxO1		
Cl 35	sensitive	Pdk1	p Pdk1	p Akt	Rictor	p Rictor	p mTOR	S6	p S6	p S6	p P70 S6			p FoxO1	Cyclin D1
Cl 41	sensitive	Pdk1	p Pdk1		Rictor		p mTOR	S6		p S6	p P70 S6	PTEN	FoxO1	p FoxO1	Cyclin D1
Cl 46	sensitive	Pdk1	p Pdk1		Rictor		p mTOR	S6		p S6	p P70 S6	PTEN	FoxO1	p FoxO1	Cyclin D1

B

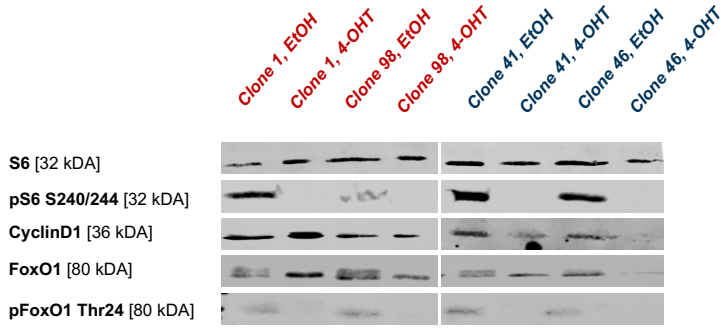

Figure 7. PI3K/Akt Signaling.

Overview of the performed western blots. **A.** Table with assessed clones and western blots with used antibodies. In the orange frame is the Pdk1 and phosphor Pdk1 on Ser241 performed with proteins obtained from all clones to confirm the Pdk1 deletion and its inactivity. **B.** Final blots of the selected antibodies and clones.

Protein levels of the cyclin D1 were higher in the resistant clones. The family of cyclins regulates the cell cycle, and the abundance of cyclin D1 promotes the progression of the cells through the G1/S phase [6].

Other blots however showed no significantly different levels of protein products throughout PI3K/Akt signaling. Especially, levels of the protein products of the FoxO family as well as of the mTORc2 (here not shown) remained similar in the sensitive and the resistant clones.

5.2 Role of SAGA and Mediator complex in *Pdk1*-depleted PDAC

This chapter describes the role of SAGA and Mediator complex in the resistance to the *Pdk1 deletion*. Using the data obtained from the genome-wide CRISPR/Cas9 knockout screen of K.Sleiman, it validates the screen results identifying the knockouts of these members to give a growth advantage to the Pdk1-deletion-resistant clones as well as the bulk cell line. The following subchapters outline the results of the validation of the genome-wide CRISPR/Cas9 knockout screen.

5.2.1 Knockout of the SAGA and Mediator members provides a growth advantage to the *Pdk1*-deletion-resistant clones

The original genome-wide CRISPR/Cas9 knockout screen identified the knockouts of the members of the SAGA and Mediator complex to provide growth to PDAC, especially to the PDAC clones with chronic resistance to the Pdk1-deletion. The CRISPR/Cac9 knockout screen is described in detail in the thesis of K. Sleiman. BRIE gene library was used in the screen.

To determine the effect of the knockout of the respective genes in the bulk cell line and the resistant clones, β-scores were calculated by F. Wang using the MAGeCKFlute pipeline. Genes showing positive β-scores, correlating with enrichment, were plotted into the STRING database by K. Sleiman. The database maps the predicted protein iterations. The experiment showed, amongst cell signaling pathways and cell cycle regulators, a cluster of enriched genes in the SAGA and Mediator complex.

Singular hits were validated in this thesis showing various levels of growth advantage in *Pdk1*-depleted PDAC cells, effect visible in both – the bulk cell line and in the PDAC single-cell clones. Amongst the top hits of the SAGA complex were Usp22 and Atxn7L3, amongst Mediator complex Med16 and Med13. Results of the STRING analysis and corresponding β-scores from the CRISPR/Cas9 knockout screen are shown in Figures 8 and 9.

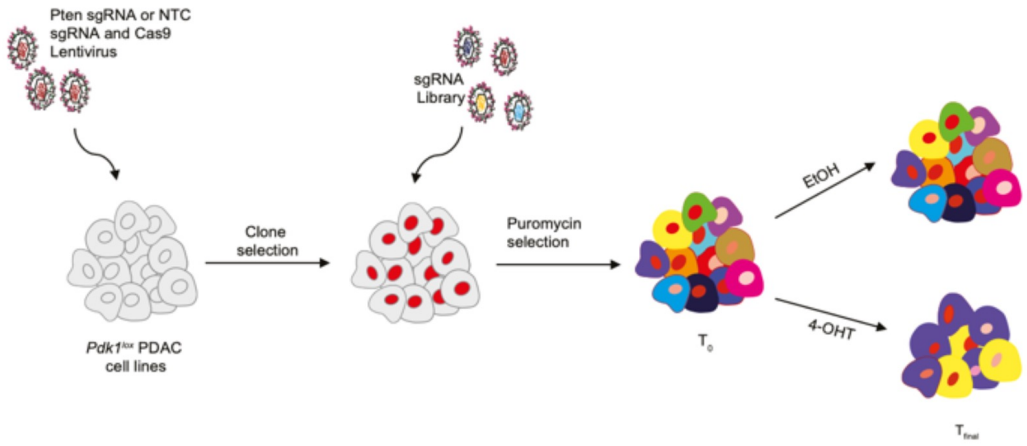

Picture 7. Genome-wide CRISPR/Cas9 knockout screen

Schematic of the CRISPR screens in the context of acute Pdk1 deletion in the CV7250 cell line (each treatment condition, EtOH and 4-0HT, was done in 2 independent replicates). For the generation of a cell line with stably expressed Cas9 components, the Cas9 components were titrated and transduced at an MOI of ≤ 0.5 and selected with 9 µg/ml Blasticidin. Selection was performed for 7 days. For the screening, the cell line was then transduced with the sgRNA library with an MOI of 0.3. The transduction was scaled up such that the sgRNA library has coverage of > 500x. 16 hours post-infection, the cells were trypsinized and seeded into 175cm flasks. 48 hours post-infection, antibiotic selection with puromycin (2,5 µg/ml) was started and carried out for 7 days. The transduced cells were divided into two groups (EtOH control and 4-OHT treatment) post-selection. The treatment was performed for 7 days and then the cells were cultured in normal media till the final timepoint. A minimum of 50 million cells was maintained throughout the culture to maintain the library representation. Cell pellets for gDNA were collected throughout various time points of the screening, with 3-day intervals, including the final time point. The final time point was collected 27 days post-selection and 20 days post-EtOH and 4-OHT treatment. Picture and description adapted from PhD thesis of K. Sleiman.

A

Gene	β_Score WT	β_Score Res
Tada1	0,24	1,22
Taf5l	0,27	1,06
Taf6l	0,39	0,94
Usp22	0,21	0,89
Supt20	0,31	0,81
Tada2b	0,33	0,66
Atxn7l3	0,09	0,51
Supt7l	0,02	0,44
Atxn7	-0,11	0,13
Tada3	-0,04	0,12
Taf9b	-0,02	0,12
Usp27x	0,13	0,09
Usp51	0,07	-0,05
Kat2a	-0,02	-0,06
Taf10	-0,55	-0,21
Eny2	-0,44	-0,35
Taf12	-0,51	-0,75

B

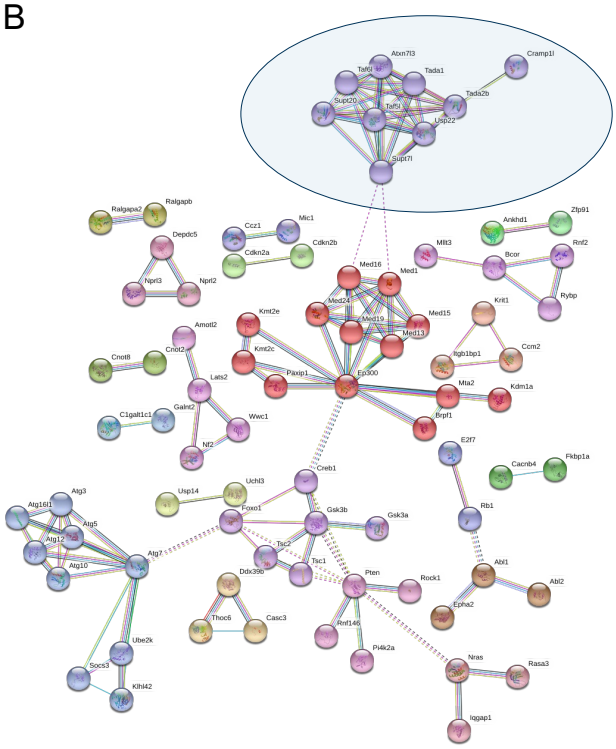

Figure 8. Hits of the CRISPR/Cas 9 knockout screen SAGA complex.

A. Single-cell clones with chronic resistance to the Pdk1-deletion (β_Score Res) and Pdk1 wild-type clones (β_Score WT) are listed in the table ranked by the β-scores from most positive to the negative. **B.** Results of the STRING analysis in the resistant clones showing the clustered hits of the SAGA complex (light blue circle). [33]

A

Gene	β_Score WT	β_Score Res
Med16	0,17	0,96
Med13	-0,32	0,74
Med15	-0,01	0,67
Med24	-0,14	0,65
Med19	-0,23	0,50
Med1	-0,25	0,41
Med12	-0,82	0,30
Med10	-0,47	0,24

B

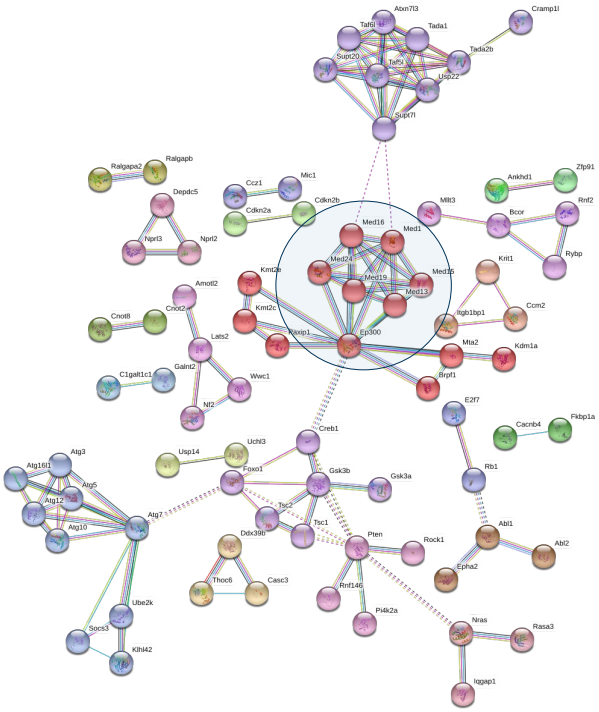

Figure 9. Hits of the CRISPR/Cas9 knockout screen. Enrichment of Mediator complex.

A. Single-cell clones with chronic resistance to the Pdk1-deletion (β_Score Res) and Pdk1 wild-type clones (β_Score WT) are listed in the table ranked by the β-scores from most positive to the negative. **B.** Results of the STRING analysis in the resistant clones showing the clustered hits of the Mediator complex (light blue circle). [33]

Genomic DNA of the CRISPR/Cas9 knockouts was isolated and sent for Sanger DNA sequencing. TIDE software was then used to determine the cutting efficiency of the respective sgRNA. Single-guide RNAs with their responding cutting efficiencies are listed in the table

Table 27. Cutting efficiencies of the sgRNAs

sgRNA	Cutting Efficiency (in percentage)
Tada1 sgRNA_1	68%
Tada1 sgRNA_4	88%
Taf5L sgRNA_1	98%
Taf5L sgRNA_3	96%
Usp22 sgRNA_1	86%
Usp22 sgRNA_2	96%
Atxn7L3 sgRNA_3	67%
Atxn7L3 sgRNA_4	91%
Med13 sgRNA_2	85%
Med13 sgRNA_3	91%
Med16 sgRNA_3	85%
Med16 sgRNA_4	-

5.2.2 Identification of the hits with the strongest resistant phenotype to the *Pdk1*-deletion

To validate the proliferation effect of the CRISPR-mediated knockouts of SAGA and Mediator complex, clonogenic assays were performed in three technical replicas. To visualize the proliferation, plates were stained with crystal violet. After the photo-documentation, a 1% SDS was applied to the plates. After 72 hours of incubation on an orbital shaker, absorbances of the plates were measured to quantify the proliferation. This quantification is shown in Figure 10. In the following step, hits with the most significant proliferation were analyzed further and are described in the following subchapters. In summary, all hits validated in this work showed proliferation despite the *Pdk1*-loss.

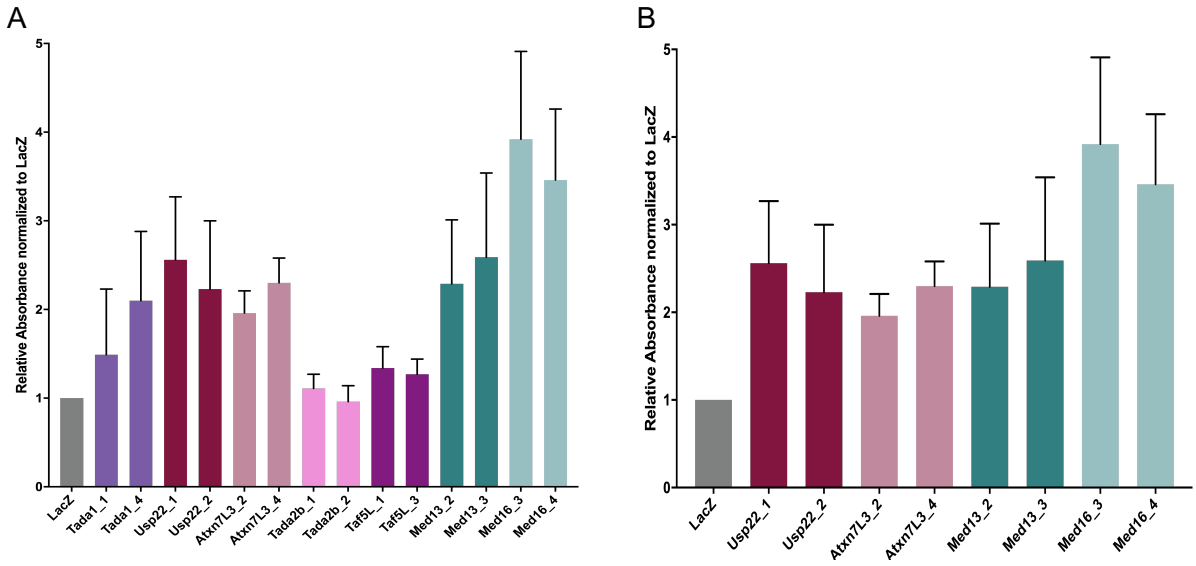

Figure 10. Relative proliferation quantification of the CRISPR/Cas9 knockout.

Colonies stained with crystal violet were solubilized with 1% SDS and incubated for 72 hours. Subsequently, the absorbances of the plates were measured. The experiment was repeated in 3 replicas (n = 3) and their absorbances normalized to the absorbance of the LacZ control. The final average values with their standard deviations were plotted in the bar graph. **A.** The absorbances of all validated hits from the genome-wide CRISPR/Cas9 knockout screen. **B.** The absorbances of the top hits with the strongest *Pdk1-deletion-resistant* phenotype. Mean ± SD, n = 3. [33]

Knockouts of *Usp22* and *Atxn7L3* genes showed the strongest proliferation phenotype within the SAGA complex

To validate the results of the genome-wide CRISPR/Cas9 knockout screen identifying the members of the SAGA complex as enriched in the Pdk1-deletion-resistant clones, clonogenic assays of the singular hits were performed. Amongst the validated genes, Usp22 and Atxn7L3 showed the most abundant proliferation in the bulk CV7250 cell line after the 4-OHT-mediated *Pdk1* deletion.

Usp22 as an enzymatically active unit of the SAGA complex functions as a histone H2B ubiquitin-hydrolase. Emerging publications analyzing Usp22 in carcinogenesis mark its role as

highly cancer- and context-dependent [14, 17]. In this work, by generating a Usp22 knockout, the tumor-suppressing role of Usp22 in PDAC was explored.

Within the SAGA complex, Atxn7L3 directs Usp22 to its substrate H2B. In their publication, Atanassov et al. [34] identified the depletion of Atxn7L3 to have a greater effect on the regulation of the levels of de-ubiquitinated H2B than Usp22.

For every gene, two single-guide RNAs with the highest enrichment in the original genome-wide CRISPR/Cas9 knockout screen were selected for the validation experiments. LacZ was used as a control. The clonogenic assays were performed in three technical replicas. Cutting efficiencies of the sgRNAs were determined as described in Chapters 4.5.5 and 4.5.6. Results are consistent for both single-guide RNAs.

To quantify the proliferation effect, crystal violet-stained clonogenic assay plates were solubilized in 1% SDS, and their absorbances were measured and plotted in bar graphs.

Western blots were used to validate the CRISPR/Cas 9 gene knockout.

Figure 11 summarizes the results of the CRISPR/Cas9-mediated knockout of the *Usp22* gene in the PDAC CV7250 epithelial cell line after 4-OHT-mediated deletion of the *Pdk1*.

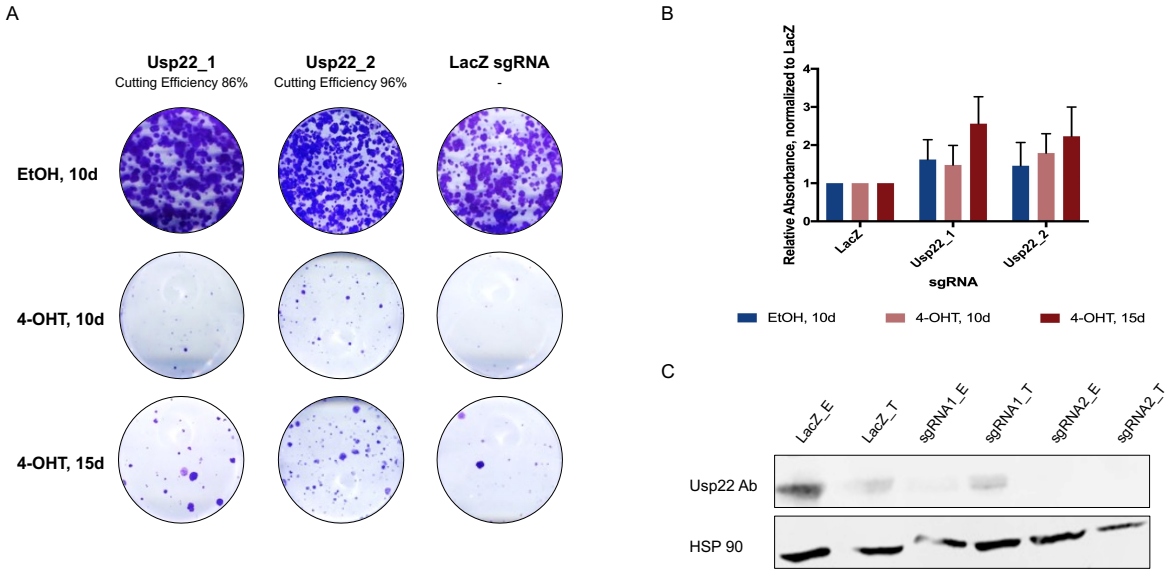

Figure 11. CRISPR/Cas 9 knockout of the Usp22 in CV7250 cell line after *Pdk1* deletion.

A. Clonogenic assays of the CRISPR/Cas9 knockouts of the Usp22 in CV7250 cells 10 and 15 days after the EtOH or 4-OHT treatment. Single-guide RNA 1 and 2. **B.** Relative absorbance of the crystal violet stained clonogenic assay plates after solubilization with 1% SDS. Mean ± SD; n = 3 technical replicas. **C.** Western blot validation of the CRISPR/Cas9 gene knockout of both single-guide RNA with HSP90 as a loading control.

Figure 12 shows the results of CRISPR/Cas9-mediated knockout of the *Atxn7L3* gene in the CV7250 cell line after the *Pdk1* deletion.

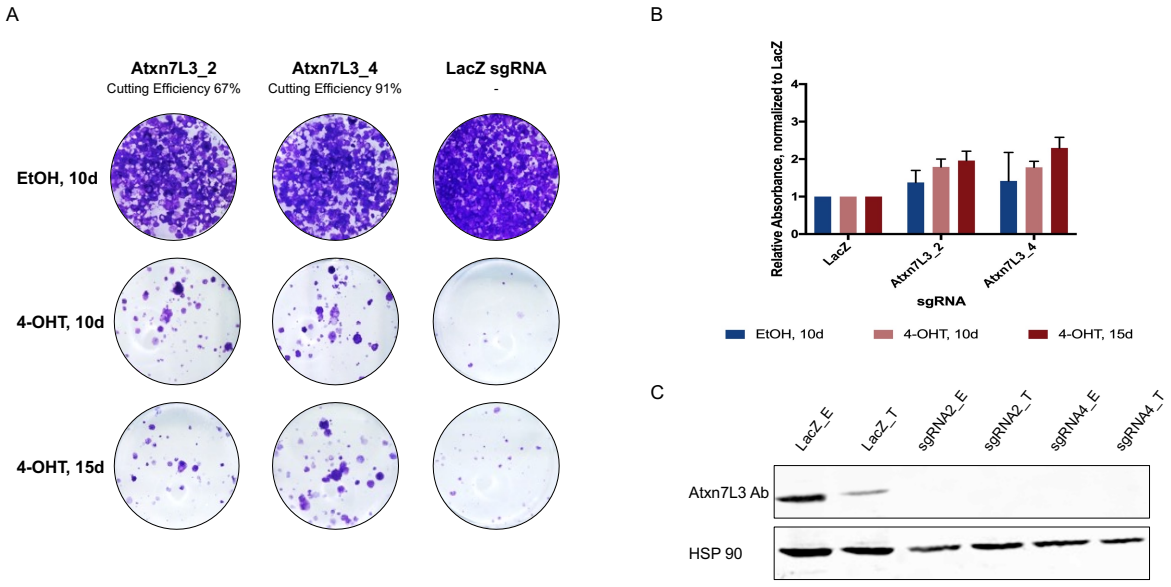

Figure 12. CRISPR/Cas 9 knockout of the Atxn7L3 in CV7250 cell line after *Pdk1* deletion.

A. Clonogenic assays of the CRISPR/Cas9 knockouts of the Atxn7L3 in CV7250 cells 10 and 15 days after the EtOH or 4-OHT treatment. Single-guide RNA 3 and 4. **B.** Relative absorbance of the crystal violet stained clonogenic assay plates after solubilization with 1% SDS. Mean ± SD; n = 3 technical replicas. **C.** Western blot validation of the CRISPR/Cas9 gene knockout of both single-guide RNA with HSP90 as a loading control.

Knockouts of *Med13* and *Med16* genes showed the strongest proliferation phenotype within the Mediator complex

The genome-wide CRISPR/Cas9 knockout screen identified two members of the Mediator complex – Med13 and Med16 to be enriched in the CV7250 PDAC bulk cells, as well as, in the resistant clones after the *Pdk1*-deletion.

Of the two Mediator members, Med16 is the lesser-researched one in the context of human carcinogenesis. Its function is to connect the Core Mediator to its Tail. Saleh et al. [21] describe the loss of Med16 to promote an unspecific transcription enhancement by disconnection of the tail to the rest of the complex. We hypothesize that one of the mechanisms of the resistance in the PDAC carcinogenesis could be due to the loss of connecting units and therefore enhancement of the enzymatic activity of the disconnected complex units.

Med13 builds together with Med12, CDK8, and Cyclin C a kinase module of the Mediator complex. The role of Med13 in human carcinogenesis is yet to be researched in detail, however, Gonzales et al. [35] link the loss of Med12 (a co-partner of Med13 in the kinase unit) to the enhanced TGFβ-signaling and in following to the enhancement of multi-drug resistance and epithelial-to-mesenchymal transition.

To validate these results, two single-guide RNAs with the highest enrichment score were selected for each gene. LacZ was used as a control. Clonogenic assays were used to determine the proliferation. They were performed in three technical replicas. Cutting efficiencies of the sgRNAs were determined as described in Chapters 4.5.5 and 4.5.6.

To visualize the proliferation, the plates with cells containing the CRISPR/Cas9 knockout were stained with crystal violet after 10 and 15 days of incubation. Med13 and Med16 showed strong proliferation effects, consistent in both single-guide RNAs.

Proliferation was quantified by measuring the absorbance of the crystal violet-stained plates/1% SDS mix. Subsequently, the raw absorbance values were normalized to the absorbance of the LacZ plates.

Western blots were used to validate the CRISPR/Cas 9 gene knockout. An exception from this is the CRISPR/Cas9-mediated knockout of the *Med16*. There is no western blot for the validation of this knockout. This point is further discussed in Chapter 6.

Figure 13 shows the effect of the Med16 knockout on the PDAC cells after the deletion of the Pdk1.

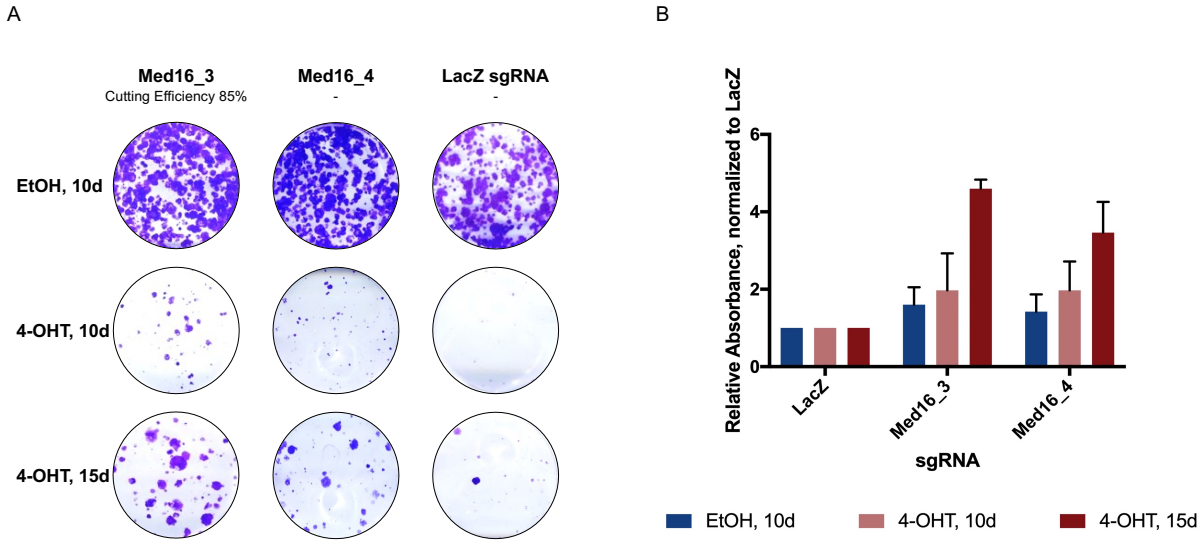

Figure 13. CRISPR/Cas 9 knockout of the Med16 in CV7250 cell line after *Pdk1* deletion.

A. Clonogenic assays of the CRISPR/Cas9 knockouts of the Med16 in CV7250 cells 10 and 15 days after the EtOH or 4-OHT treatment. Single-guide RNA 3 and 4. **B.** Relative absorbance of the crystal violet stained clonogenic assay plates after solubilization with 1% SDS. Mean ± SD; n = 3 technical replicas.

Figure 14 shows the effect of the Med13 knockout on the PDAC CV7250 bulk cell line after the *Pdk1 deletion*.

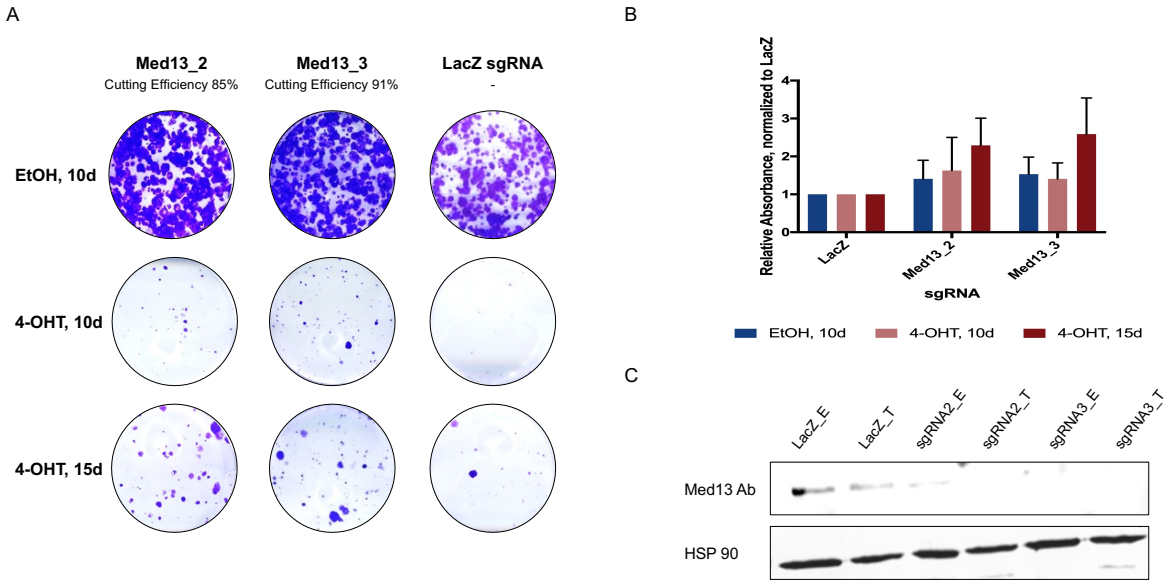

Figure 14. CRISPR/Cas 9 knockout of the Med13 in CV7250 cell line after *Pdk1* deletion.

A. Clonogenic assays of the CRISPR/Cas9 knockouts of the Med13 in CV7250 cells 10 and 15 days after the EtOH or 4-OHT treatment. Single-guide RNA 2 and 3. **B.** Relative absorbance of the crystal violet stained clonogenic assay plates after solubilization with 1% SDS. Mean ± SD; n = 3 technical replicas. **C.** Western blot validation of the CRISPR/Cas9 gene knockout of both single-guide RNA with HSP90 as a loading control [33].

5.2.3 Gene set differential expression analysis of SAGA and Mediator complex CRISPR/Cas9 knockouts

We performed RNA sequencing as described in Chapters 4.3.4 and 4.3.5 to investigate the differences in the transcriptional level between CRISPR/Cas9-mediated gene knockouts of SAGA and Mediator complex and LacZ controls after *Pdk1*-deletion. The bioinformatical analysis used in this work was performed by F. Wang. To visualize differentially expressed genes we used a volcano plot (performed by K. Sleiman). Gene set enrichment analysis (GSEA) was used to represent differentially expressed hallmarks [36–38].

Results of the gene set enrichment analysis of the SAGA and Mediator complex are shown in Figure 15. Hallmarks significantly up- (red bars) and down-regulated (blue bars) with corresponding adjusted p-value < 0,05 were included in the figure.

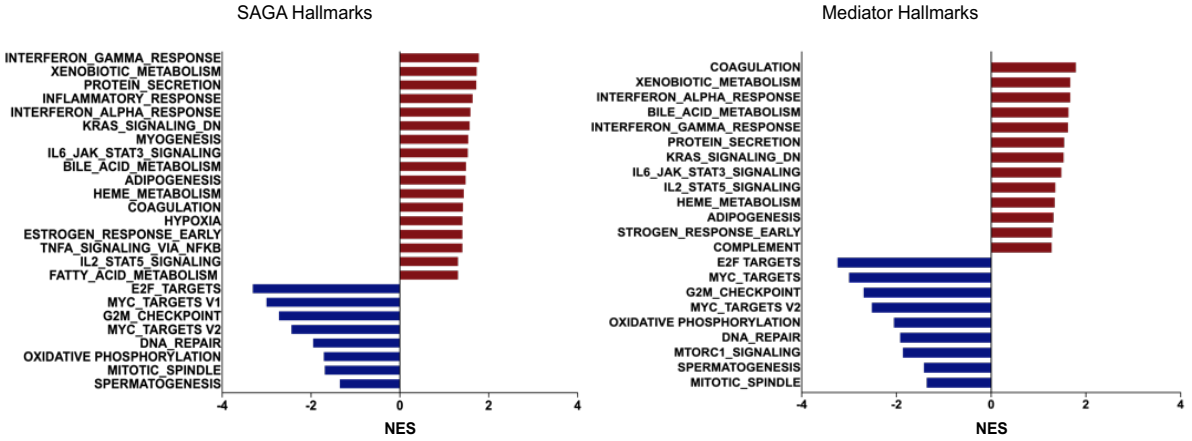

Figure 15. Gene set enrichment analysis of SAGA and Mediator complex.

Gene set enrichment analysis with significantly differentially expressed hallmark pathways using MSigDB [38]. Red bars represent significantly upregulated pathways in the CRISPR/Cas9-mediated knockout cells, and blue bars represent significantly downregulated pathways. The X-axis stands for normalized enrichment score (NES), adjusted p-value < 0,05.

The results of the GSEA analysis of both complexes showed a significant upregulation of the xenobiotic metabolism-involved genes. Usp22 as well as several members of SAGA and Mediator are repeatedly investigated in the context of multiple drug resistance. The results of this analysis follow the previous publications as genes regulating xenobiotic metabolism are major players in drug metabolism [39].

Interestingly we observed upregulation of hallmarks of inflammatory response – Interferon alpha, Interferon gamma, and IL6/JAK/STAT3 signaling suggesting an upregulation of the inflammatory processes in the *Pdk1*-deletion resistant PDAC cells.

E2F Targets, DNA Repair Genes as well as G2M Checkpoint are hallmarks in which knockouts of both, SAGA, and Mediator Complexes, showed a significant downregulation. These findings suggest that aberrant transcription and cell cycle deregulation play a major role in the resistance of the PDAC cells independent of Pdk1.

Volcano plots performed by K. Sleiman were used to visualize significantly up- and downregulated genes in SAGA and Mediator knockout cells in respect to the controls. The results are shown in Figure 16. Following the GSEA analysis of the hallmarks which identified hallmark JAK-STAT signaling to be upregulated in the CRISPR/Cas9-mediated SAGA knockouts. Socs3, an important regulator of the JAK-STAT signaling is amongst upregulated genes in SAGA complex knockouts. Similarly, Muc1, another gene overexpressed in SAGA knockouts and JAK-STAT signaling regulator has been reported to play a role in drug and radiotherapy of tumors of the upper gastrointestinal tract including pancreatic cancer [40].

Several genes reported in the context of carcinogenesis were overexpressed in knockouts of the Mediator complex. Consistent with previous publications Nupr1 was overexpressed. Nupr1 was reported to relate to multiple drug resistance as well as aggressive cancer phenotype [41].

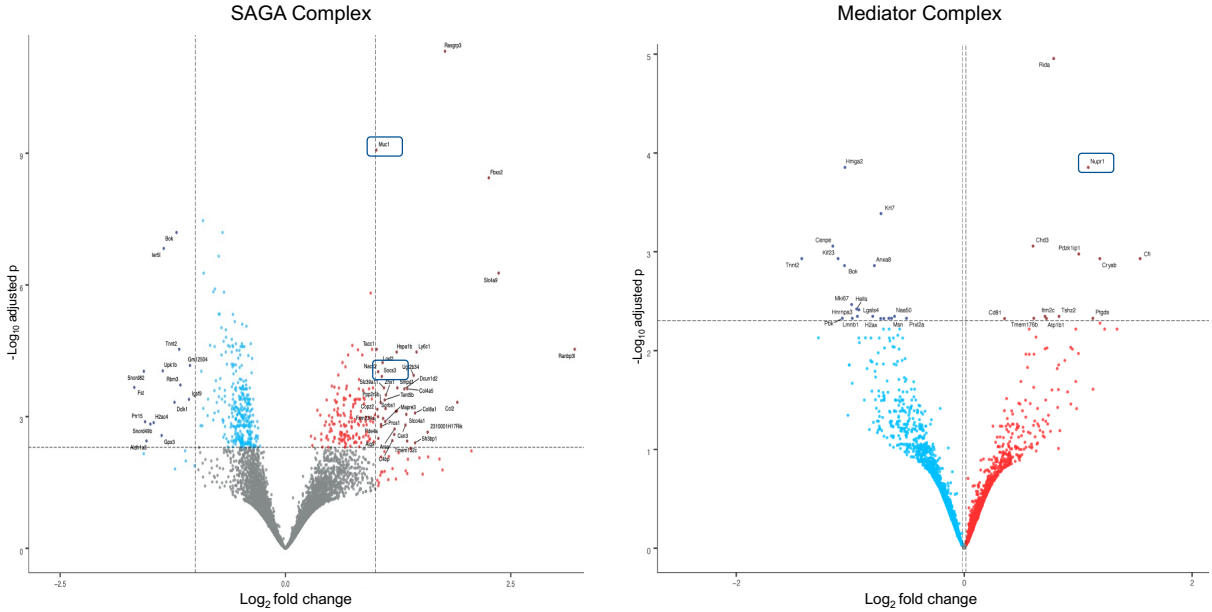

Figure 16. Volcano plot of the SAGA and Mediator complex knockouts.

Volcano showing differentially expressed genes in comparison SAGA complex knockouts versus LacZ control (left) and Mediator complex knockouts versus LacZ control (right) after 4-OHT-mediated *Pdk1*-deletion. Significantly (padj = 0,005) up- or downregulated genes are represented with red (for upregulated) and blue (for downregulated) color. Blue framed are genes mentioned above. The X-axis represents the -Log_{10} adjusted p, the Y-axis the Log_2fold change, p adj = 0,005.

5.3 Effect of the CRISPR/Cas9 SAGA and Mediator knockouts in the single-cell PDAC clones

This chapter describes the role of the SAGA and Mediator complex in the single-cell clones with acute resistance to *Pdk1 deletion*. These experiments were performed to obtain further insight into the role of the complexes in the acute resistance to the Pdk1-loss. CRISPR/Cas9-mediated knockouts with the strongest resistant phenotype in the bulk PDAC cell line experiments were also performed on resistant clone 19 and sensitive clone 7 (see Chapter 5.1).

Following the results in the CV7250 bulk cell line showed Usp22 and Med16 the strongest proliferation independent of the Pdk1. Figure 17 shows the results of the clonogenic assays for Usp22 and Med16 in resistant clone 19 and in sensitive clone 7.

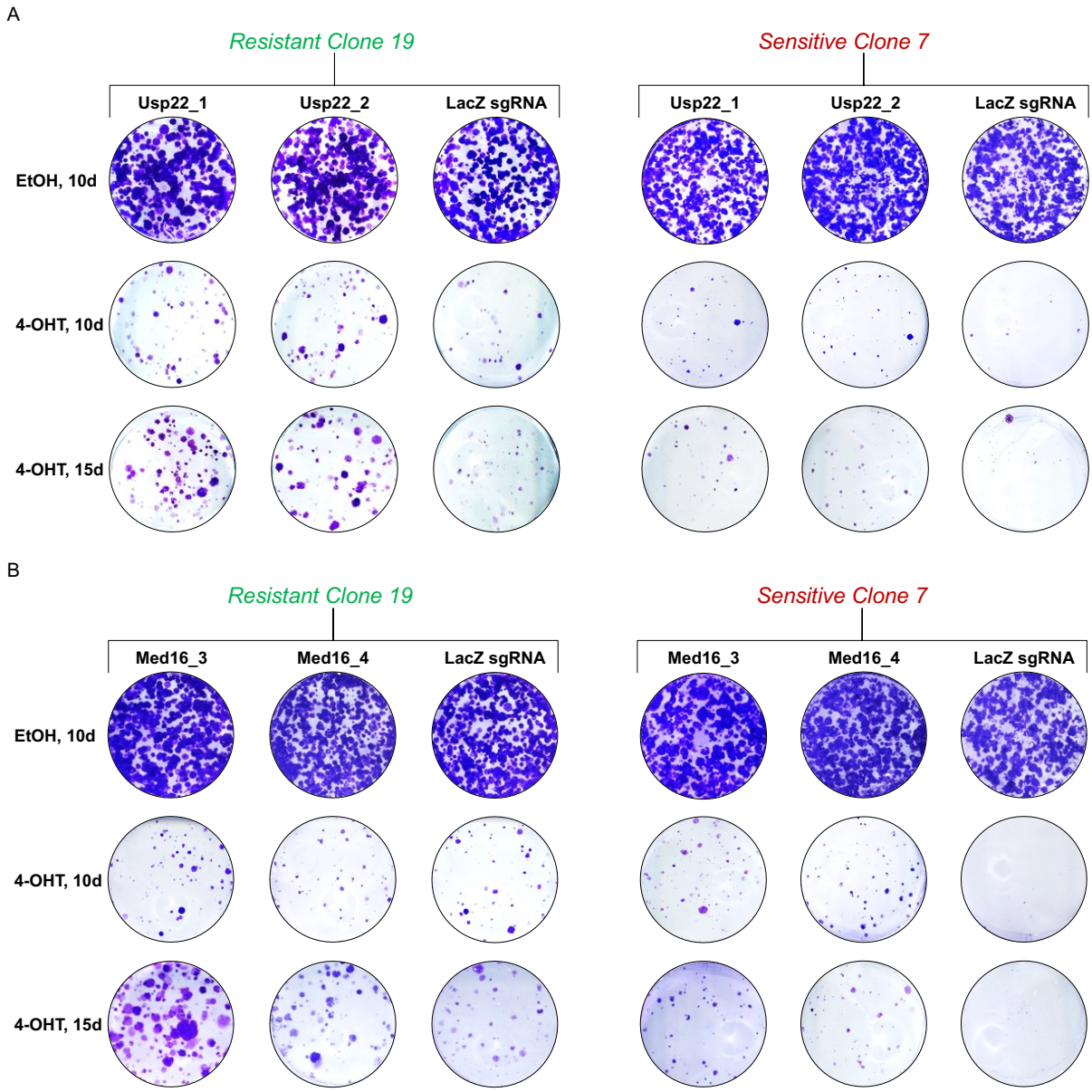

Figure 17. Clonogenic assay of the top hits in PDAC single-cell clones.

The experiment with resistant clone 19 was performed in three seedings to obtain three technical replicates. An experiment with sensitive clone 7 was performed in one seeding, and three replicates within the seeding. Generated CRISPR knockouts were treated with 600 nM 4-OHT or EtOH for 7 days, re-seeded, and incubated for 10 (EtOH and 4-OHT) and 15 days (4-OHT). Afterwards, plates were stained with crystal violet. **A.** Knockouts of Usp22 sgRNA 1 and sgRNA 2 in resistant clone 19 and sensitive clone 7. Ethanol controls (first row), 10 days (second row), and 15 days (third row) after 4-OHT-mediated *Pdk1*-deletion [33]. **B.** Knockouts of Med16 sgRNA 3 and sgRNA 4 in resistant clone 19 and sensitive clone 7. Ethanol controls (first row), 10 days (second row), and 15 days (third row) after 4-OHT-mediated *Pdk1*-deletion. [33]

Quantification of the proliferation was performed by measuring the absorbances of the crystal violet-stained plates solubilized in 1% SDS. The absorbances were plotted in the bar graph. The results are shown in Figure 18. To compare the proliferation of the CRISPR/Cas9-

mediated knockouts of the resistant and sensitive clone, the corresponding absorbances of both - clone 7 and clone 19 were plotted together in a bar graph. Partially lower proliferation of the knockouts in comparison to the LacZ control in clone 7 is due to the insufficient PBS wash of the LacZ 4-OHT after 15 days plate resulting in the falsely high absorbance values.

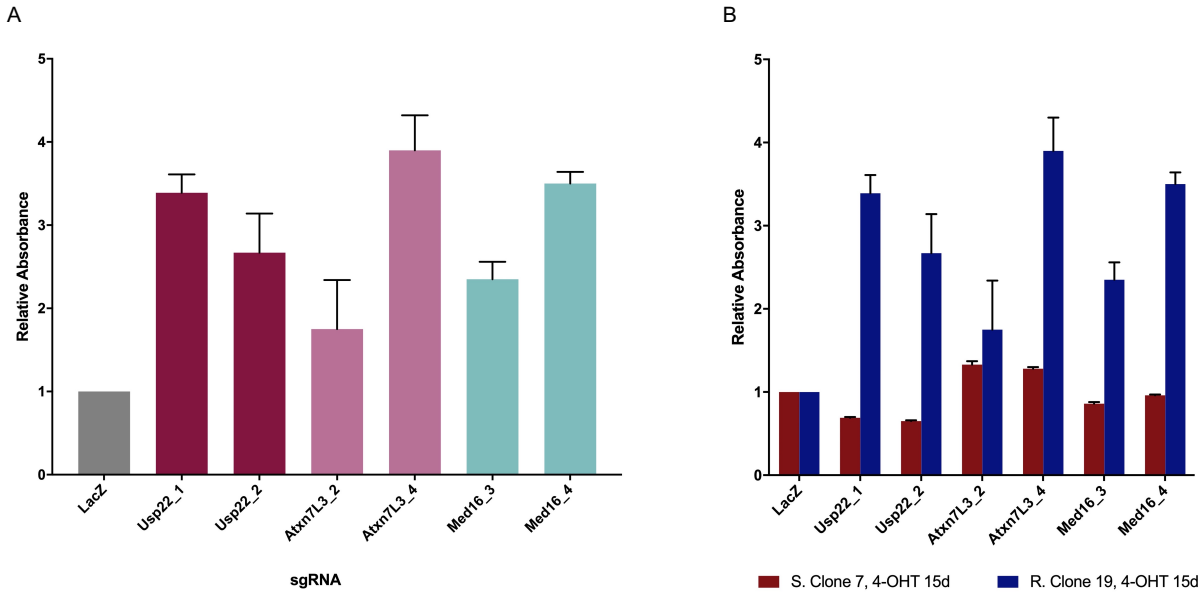

Figure 18. Proliferation quantification of the CRISPR/Cas9 knockouts in the clones.

Crystal violet-stained plates were solubilized in 1% SDS solution and incubated for 72 hours. Final absorbances were then measured and plotted in bar graphs. Clone 19 in three technical replicas n = 3, clone 7 in one replica n = 1. **A.** Bar graph of the absorbances of the CRISPR/Cas9-mediated knockouts 15 days after 600 nM 4-OHT treatment relative to the LacZ in the resistant clone 19. **B.** Bar graph of the absorbances of the CRISPR/Cas9-mediated knockouts relative to LacZ, comparison between resistant clone 19 (blue) and sensitive clone 7 (red).

6 Discussion and outlook

Despite broad research worldwide, PDAC remains one of the deadliest cancers with a devastating prognosis for patients and a therapeutic challenge for medical professionals. A variety of multimodal therapeutic approaches has been researched in the last decades. Since mutant KRAS is known to be altered in more than 90% of the PDAC, it naturally became the most investigated target. Nevertheless, most attempts to target KRAS were in vain as the gene disposes of many drug-evasive mechanisms. Even though the alleged drug resistance of the KRAS went through a breakthrough in the last years, the research remains focused on the downstream KRAS effects as well. One of these effectors is Pdk1. Previous works of the group of Prof. Saur that are described in earlier chapters of this work proved that even though the majority of PDAC cells show an impaired proliferation in the lack of Pdk1, a small subpopulation proliferates independent of the Pdk1. To investigate why, is of utmost importance if the targeted cancer therapies are to be developed for the PDAC patients.

6.1 Role of *Pdk1* deletion in PDAC maintenance

A dual recombinase mouse model developed in the lab of Prof. Saur enabled this project to mimic the tumor initiation and maintenance of the $KRAS^{G12D}$-driven PDAC. By floxing the Pdk1 in already developed PDAC tumors the research group recapitulated the important hallmarks of the carcinogenesis and observed almost complete impairment of the cancer cell proliferation. To further characterize the minor cell subpopulation of PDAC cells which continued proliferating despite successful *Pdk1* deletion, in this work, single-cell clones of the PDAC CV7250 cell line were generated. Then, the tamoxifen-mediated *Pdk1* deletion was generated and the post-deletion clone proliferation was analyzed. From over one hundred isolated clones 9% continued growing, albeit at a slower pace.

6.2 PI3K/Akt signaling in the resistance to *Pdk1* deletion

PI3K/Akt signaling is a major signaling pathway in the initiation, development, and maintenance of many cancer types. By inhibition of the FoxO family and of *p53* it regulates apoptosis, through mTORC1, TSC1, and TSC2 it regulates protein synthesis, through CDKs and cyclins it regulates the cell cycle. Therefore, one of the first initial approaches was to investigate the differences between *Pdk1*-deletion-resistant and -sensitive clones in the PI3K/Akt signaling[5] [3].

In this research, a broad western blot analysis of the PI3K signaling was performed. In the focus were the cyclins, mTORC2 complex members as well as metabolic regulators.

The performed analysis showed a relative consistency of protein function of the respective members of the PI3K/Akt signaling pathway with no significant reproducible difference between resistant and sensitive clones. A possible explanation is, that the analysis was performed on clones with acute resistance to the Pdk1 loss. K. Sleiman generated in her research clones with chronic resistance against Pdk1-loss. Those clones were cultured for a longer time and showed a higher proliferation rate as shown in Figure 19.

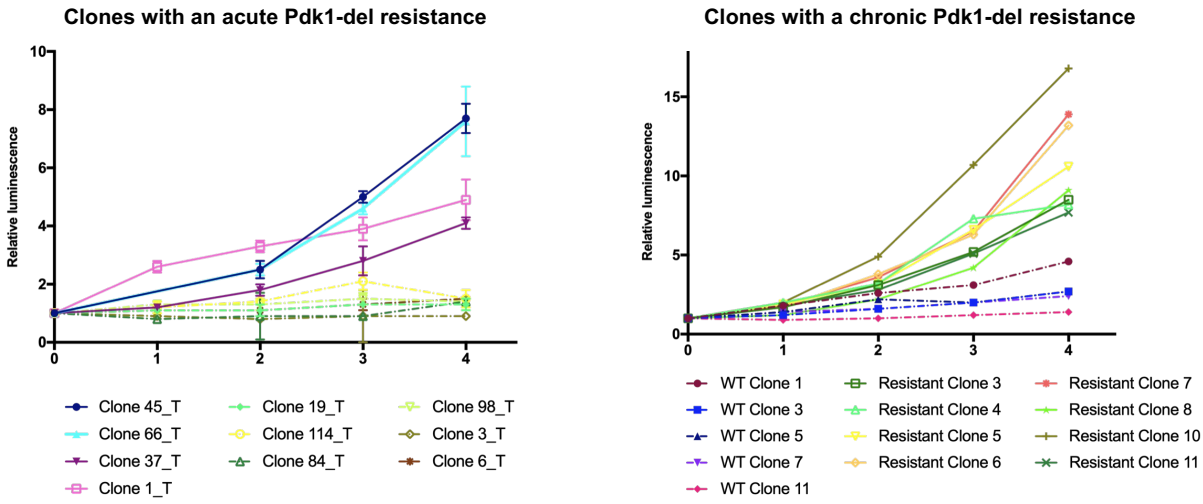

Figure 19. Acute versus chronic Pdk1 deletion resistance.

Clones were treated for 7 days with 4-OHT to induce Pdk1 deletion. Ethanol was used as a control. 500 cells/well were seeded in the following step and incubated for 1 to 5 days. Cell titer glo was added and luminescence was measured. The first measurement was performed 24 hours after seeding and used as a normalization – day 0. To visualize the proliferation of PDAC clones in the first 4 days after Pdk1 deletion the luminescence relative to day 0 was plotted in XY graph. Clones with chronic resistance against Pdk1 deletion (right graph) are showing a higher proliferation rate.

Observing a higher proliferation rate of the clones with chronic resistance to the *Pdk1* deletion, in the future projects a broadening of the PI3K/Akt signaling analysis on those clones as well as the comparison between clones with acute and chronic resistance to determine potential alterations in the signaling after longer incubation time and longer persisting resistance should be performed in a detailed manner.

6.3 RAS/Erk pathway as a cross interactor to PI3K/Akt signaling

As Mendoza et al. [42] describe, both PI3K/Akt and RAS/Erk signaling pathways are major regulators of cellular mechanisms including proliferation, metabolism regulation, and cell cycle

regulation. There are many cross-reactors responsible for the inhibition or activation of the respective pathways. One of them is TCS2 and mTORC1 through which the RAS/Erk pathway cross inhibits the activity of PI3K/Akt.

To understand the differences between acute and chronic resistance to the *Pdk1* deletion as well as the acute resistance per se, the pathway analysis should be further broadened to research the key interaction points between two signaling pathways in a more controlled manner.

6.4 Genome-wide CRISPR/Cas9 knockout screen to identify resistance to *Pdk1* deletion in PDAC

PDAC carcinogenesis and its important hallmarks have been recapitulated and described quite successfully, amongst others, by other members of the research group of Prof. Saur. Nevertheless, anchors for the development of novel therapeutic strategies are scarce so far. It has become clear with time, that broader genome-wide approaches must be undertaken to achieve the required progress in targeted therapies development.

Discovery, optimization of accuracy, as well as the low costs of CRISPR/Cas technology, have enabled scientists to describe the alterations under the condition of the *Pdk1* deletion, genome-wide. By performing a screen in bulk PDAC cell line, as well as on the clones with chronic resistance to *Pdk1* deletion, K. Sleiman was able to identify various genes enriched upon *Pdk1* deletion. Amongst these genes were members of SAGA and Mediator complexes, which led to the hypothesis that their depletion might lead to the growth advantage of the PDAC in the absence of the Pdk1.

6.4.1 Knockouts of SAGA and Mediator complex

Using the data obtained from the genome-wide CRISPR/Cas9 knockout screen, I performed validation experiments of the genes that showed the highest enrichment score in the bulk PDAC cells and in the *Pdk1*-deletion-resistant clones. Amongst the top hits of the screen were *Usp22, Atxn7L3, Med13,* and *Med16*. Cancer cells obtaining the knockouts of these genes showed the strongest proliferation phenotype after *Pdk1* deletion.

With proliferation assays I detected a significant proliferation of the cells with the CRISPR/Cas9-mediated knockouts of the above-mentioned genes in comparison to the LacZ control. Cutting efficiency of above 80% infected cells was determined in all selected sgRNA using Sanger sequencing. The validation of knockout success was determined using a western blot. All knockouts except for *Med16* showed adequate results in this regard. *Med16* is commented on in a separate Subchapter 6.4.1.

To complete the analysis and to gain further insights, I would propose to perform combined CRISPR knockouts (Atxn7L3 with Usp22 and Med 13 with Med16) parallel to the singular knockouts of the SAGA and Mediator members. Since multiple interactions within these genes were reported in the past, there is a high probability, that the gain of resistance is due to the more complex aberrant activity within transcription complexes [22, 34, 35].

Usp22

Usp22 is generally referred to as one of the eleven “death from cancer genes signature” associated with poor patient prognosis, aggressive distant metastasis, and enhanced multiple cancer drug resistance [15, 16]. As research boomed and publications emerged, it has become clear, that the role of *Usp22* is highly tumor-type and -context-specific [17]. Previous publications describe the tumor suppressive as well as the oncogenic role of *Usp22* in PDAC [17]. The novelty of this thesis is in the characterization of the function of *Usp22* in the specific context of resistance against *Pdk1* deletion. With proliferation assays, I was able to show, that the knockout of the *Usp22* gene enhances the PDAC proliferation in the context of *Pdk1* deletion.

The hypothesis regarding the mechanism responsible for such a growth advantage remains open. For instance, the main role of the DUB module of the SAGA complex and its protagonist, *Usp22*, is the regulation of the histone H2B (H2Bub1). Western blots were performed to determine the protein levels of the de-ubiquitinated histone H2B and histone H2B between CRISPR knockouts and LacZ controls. There was no significant difference observed in those experiments. Nevertheless, by the small molecular weight of the target proteins, I would propose to repeat the experiment in a more controlled manner with alternative gel concentration or choose a different approach such as qPCR.

Atxn7L3

Atxn7L3 is one of the structural elements of the DUB module of SAGA. Interestingly, [34] observed that the depletion of Usp22 has a lesser effect on the H2Bub1 level than the depletion of *Atxn7L3* and its module co-partner *ENY2*. In case the main hypothesis of the resistance mechanisms against *Pdk1* deletion would be the H2Bub1 dysregulation in the absence of *Usp22,* a combined *ENY2* and *Atxn7L3* CRISPR knockout should be generated to examine their reported co-dependent role in the context of H2Bub1 regulation.

Med13

Med13, together with Med12, CKD8, and Cyclin C, is part of the kinase module of the Mediator complex [20, 22]. Equivalent to the DUB Module of the SAGA complex, also within Mediator one of the top hits is part of the enzymatically active unit of the transcription complex. The recently published work of [43] shows a Cyclin D1-modulated enhancement of resistance to alkylation in Med13-depleted cells. In concordance, by stabilization of the cellular Med13 levels, a significantly improved response to the alkylating drugs (such as platin-containing drugs) was observed. At this point, I would suggest a further analysis of the levels of the Cyclin D1 in *Med13*-knockouts in the context of the *Pdk1* deletion as well as validation of the hypothesis of [43] with a drug screen.

Med16

The role of Med16 is to connect the tail Mediator to its core part. The hypothesis is, that the enhanced resistance to the *Pdk1* deletion in the Med16-depleted cells, is due to an enhanced transcription activity of the tail caused by the loss of the regulating core part of the Mediator complex [21]. In concordance with this, in my work, I observed the strongest proliferation after

Pdk1 deletion in the Med16-depleted cells. Med16 knockouts in the clones with resistant and sensitive phenotypes to the Pdk1 corresponded to those in the bulk PDAC cell line.

The problem I faced in the course of my work was in the validation of the CRISPR/Cas9 gene knockout with western blot. In repetitive experiments, I could not detect Med16 protein either in the LacZ or in the Med16 knockouts with either of the sgRNA. Therefore, I recommend an alternative validating approach using qPCR.

6.5 Final Conclusions

In the project of my medical doctoral thesis, I followed the data obtained by C. Veltkamp and K. Sleiman in their PhD Thesis. The starting point was the knowledge of the significant role of Pdk1 in PDAC carcinogenesis. Upon tamoxifen-mediated *Pdk1* deletion, an almost complete tumor progression blockage was observed. Yet, a minor cell subpopulation continues to proliferate independent of the Pdk1, due to which mechanisms are unclear. In my project, I analyzed the aspects of the acute resistance to the *Pdk1*-deletion – in a broad manner as well as targeted on several promising genes.

I generated single-cell clones of the CV7250 PDAC cell line, treated them with tamoxifen to induce the *Pdk1 deletion*, and screened them for acute resistance. Clones that continued proliferating after the *Pdk1 deletion* were analyzed on multiple levels. I performed a broad western blot analysis of the PI3K/Akt signaling pathway and the RNA sequencing to describe differentially expressed genes and hallmarks. This thesis lists those findings and describes their possible implications in PDAC carcinogenesis.

Apart from the broad resistance analysis, a targeted search for the genes partaking in the resistance to Pdk1 deletion was conducted. K. Sleiman performed a genome-wide CRISPR/Cas9 knockout screen which she analyzed and described in her PhD thesis. Amongst other hits, this screen identified members of the SAGA and Mediator complex to be enriched in the CV7250 bulk cell line and the clones with the resistance to the *Pdk1 deletion*. In my thesis, I performed a validation of these results. I analyzed whether there is an enhanced cell proliferation upon the CRISP/Cas9-mediated knockout and after the *Pdk1 deletion*. I tested whether the enhanced proliferation upon the knockout is reproducible in three technical replicates. I quantified the proliferation taking the unspecific LacZ knockouts as a control. I performed RNA sequencing and analyzed the differentially expressed hallmarks and genes. Finally, I summarized the results and explained their implications for PDAC carcinogenesis.

In the final part of my project, I selected one clone with the strongest phenotype of resistance to the *Pdk1 deletion* and one clone with the most impaired proliferation after the *Pdk1 deletion*. I analyzed the effect of the most promising hits from the validation experiments.

7 Acknowledgments

I would like to thank Prof. Dieter Saur for allowing me to work on my medical doctoral thesis in his lab as well as for his being as for being my main supervisor throughout my thesis. I thank PD Dr. Günter Schneider for mentoring my project with valuable feedback and input. I thank Dr. Katia Sleiman for being my PhD mentor, and educating me in laboratory methods, CRISPR/Cas9 genome editing as well as theoretical backroad. I thank her for sharing the data of her CRISPR/Cas9 screen and thus giving me a basis for my experiments. I thank Fengchong Wang for performing the bioinformatical analysis. I also thank Dr Christian Veltkamp, for the generation of the cell line used in this thesis. Additionally, I would like to thank Rupert Öllinger for sequencing and the staff of the core facility of TranslaTUM. I thank Asia Madej, Bianca Thedorescu, and Dr. Tânia Custodio Santos from the AG Saur for their support in the lab as well as their feedback throughout the thesis as well as all the team of the AG Saur for their help in the lab.

I would also like to thank my parents for their immense support throughout my education and for their feedback as uninvolved medical professionals. Last, but not least, I thank Lorenzo for his unlimited help, know-how, and wit.

List of pictures

List of figures

List of tables

References

[1] N. Schönhuber *et al.,* "A next-generation dual-recombinase system for time- and host-specific targeting of pancreatic cancer," (in eng), *Nature medicine*, vol. 20, no. 11, pp. 1340–1347, 2014, doi: 10.1038/nm.3646.

[2] S. Mueller *et al.,* "Evolutionary routes and KRAS dosage define pancreatic cancer phenotypes," (in eng), *Nature*, vol. 554, no. 7690, pp. 62–68, 2018, doi: 10.1038/nature25459.

[3] S. F. Bannoura *et al.,* "Targeting KRAS in pancreatic cancer: new drugs on the horizon," (in eng), *Cancer metastasis reviews*, vol. 40, no. 3, pp. 819–835, 2021, doi: 10.1007/s10555-021-09990-2.

[4] K. Z. Thein, A. B. Biter, and D. S. Hong, "Therapeutics Targeting Mutant KRAS," (in eng), *Annual review of medicine*, vol. 72, pp. 349–364, 2021, doi: 10.1146/annurev-med-080819-033145.

[5] P. Liu, H. Cheng, T. M. Roberts, and J. J. Zhao, "Targeting the phosphoinositide 3-kinase pathway in cancer," (in eng), *Nature reviews. Drug discovery*, vol. 8, no. 8, pp. 627–644, 2009, doi: 10.1038/nrd2926.

[6] F. I. Montalto and F. de Amicis, "Cyclin D1 in Cancer: A Molecular Connection for Cell Cycle Control, Adhesion and Invasion in Tumor and Stroma," (in eng), *Cells*, vol. 9, no. 12, 2020, doi: 10.3390/cells9122648.

[7] R. J. DeBerardinis and N. S. Chandel, "We need to talk about the Warburg effect," (in eng), *Nature metabolism*, vol. 2, no. 2, pp. 127–129, 2020, doi: 10.1038/s42255-020-0172-2.

[8] P. Duda *et al.,* "Targeting GSK3 and Associated Signaling Pathways Involved in Cancer," (in eng), *Cells*, vol. 9, no. 5, 2020, doi: 10.3390/cells9051110.

[9] D. Ren, Y. Sun, D. Li, H. Wu, and X. Jin, "USP22-mediated deubiquitination of PTEN inhibits pancreatic cancer progression by inducing p21 expression," (in eng), *Molecular oncology*, vol. 16, no. 5, pp. 1200–1217, 2022, doi: 10.1002/1878-0261.13137.

[10] J. G. Doench, "Am I ready for CRISPR? A user's guide to genetic screens," (in eng), *Nature reviews. Genetics*, vol. 19, no. 2, pp. 67–80, 2018, doi: 10.1038/nrg.2017.97.

[11] D. M. Thurtle-Schmidt and T.-W. Lo, "Molecular biology at the cutting edge: A review on CRISPR/CAS9 gene editing for undergraduates," (in eng), *Biochemistry and molecular biology education : a bimonthly publication of the International Union of Biochemistry and Molecular Biology*, vol. 46, no. 2, pp. 195–205, 2018, doi: 10.1002/bmb.21108.

[12] L. Wang and S. Y. R. Dent, "Functions of SAGA in development and disease," (in eng), *Epigenomics*, vol. 6, no. 3, pp. 329–339, 2014, doi: 10.2217/epi.14.22.

[13] H. Wang, C. Dienemann, A. Stützer, H. Urlaub, A. C. M. Cheung, and P. Cramer, "Structure of the transcription coactivator SAGA," (in eng), *Nature*, vol. 577, no. 7792, pp. 717–720, 2020, doi: 10.1038/s41586-020-1933-5.
[14] R. L. Kosinsky *et al.,* "USP22-dependent HSP90AB1 expression promotes resistance to HSP90 inhibition in mammary and colorectal cancer," (in eng), *Cell death & disease*, vol. 10, no. 12, p. 911, 2019, doi: 10.1038/s41419-019-2141-9.
[15] G. V. Glinsky, "Death-from-cancer signatures and stem cell contribution to metastatic cancer," (in eng), *Cell cycle (Georgetown, Tex.)*, vol. 4, no. 9, pp. 1171–1175, 2005, doi: 10.4161/cc.4.9.2001.
[16] G. V. Glinsky, O. Berezovska, and A. B. Glinskii, "Microarray analysis identifies a death-from-cancer signature predicting therapy failure in patients with multiple types of cancer," (in eng), *The Journal of clinical investigation*, vol. 115, no. 6, pp. 1503–1521, 2005, doi: 10.1172/JCI23412.
[17] R. L. Kosinsky *et al.,* "USP22 exerts tumor-suppressive functions in colorectal cancer by decreasing mTOR activity," (in eng), *Cell death and differentiation*, vol. 27, no. 4, pp. 1328–1340, 2020, doi: 10.1038/s41418-019-0420-8.
[18] Z. C. Poss, C. C. Ebmeier, and D. J. Taatjes, "The Mediator complex and transcription regulation," (in eng), *Critical reviews in biochemistry and molecular biology*, vol. 48, no. 6, pp. 575–608, 2013, doi: 10.3109/10409238.2013.840259.
[19] W. F. Richter, S. Nayak, J. Iwasa, and D. J. Taatjes, "The Mediator complex as a master regulator of transcription by RNA polymerase II," (in eng), *Nature reviews. Molecular cell biology*, vol. 23, no. 11, pp. 732–749, 2022, doi: 10.1038/s41580-022-00498-3.
[20] O. Luyties and D. J. Taatjes, "The Mediator kinase module: an interface between cell signaling and transcription," (in eng), *Trends in biochemical sciences*, vol. 47, no. 4, pp. 314–327, 2022, doi: 10.1016/j.tibs.2022.01.002.
[21] M. M. Saleh, C. Jeronimo, F. Robert, and G. E. Zentner, "Connection of core and tail Mediator modules restrains transcription from TFIID-dependent promoters," (in eng), *PLoS genetics*, vol. 17, no. 8, e1009529, 2021, doi: 10.1371/journal.pgen.1009529.
[22] S. Huang *et al.,* "MED12 controls the response to multiple cancer drugs through regulation of TGF-β receptor signaling," (in eng), *Cell*, vol. 151, no. 5, pp. 937–950, 2012, doi: 10.1016/j.cell.2012.10.035.
[23] P. Corporation, "CellTiter-Glo Luminescent Cell Viability Assay Technical Bulletin #TB288,"
[24] K. Mullis, F. Faloona, S. Scharf, R. Saiki, G. Horn, and H. Erlich, "Specific enzymatic amplification of DNA in vitro: the polymerase chain reaction," (in eng), *Cold Spring Harbor symposia on quantitative biology*, 51 Pt 1, pp. 263–273, 1986, doi: 10.1101/sqb.1986.051.01.032.
[25] Blesilda Adlaon - QIAGEN, "HB-0435-007_HB_RNYMini_0623_WW,"
[26] Le Cong and F. Zhang, "Genome engineering using CRISPR-Cas9 system," (in eng), *Methods in molecular biology (Clifton, N.J.)*, vol. 1239, pp. 197–217, 2015, doi: 10.1007/978-1-4939-1862-1_10.
[27] "Instruction-NucleoBond-Xtra,"
[28] "Mammalian Genomic DNA Miniprep Kit,"
[29] E. K. Brinkman and B. van Steensel, "Rapid Quantitative Evaluation of CRISPR Genome Editing by TIDE and TIDER," in pp. 29–44.
[30] New England Biolabs, "Monarch PCR & DNA Cleanup Kit (5 µg) T1030 manual,"

[31] J. Park, J. Cho, and E. J. Song, "Ubiquitin-proteasome system (UPS) as a target for anticancer treatment," (in eng), *Archives of pharmacal research*, vol. 43, no. 11, pp. 1144–1161, 2020, doi: 10.1007/s12272-020-01281-8.
[32] L. D. Fricker, "Proteasome Inhibitor Drugs," (in eng), *Annual review of pharmacology and toxicology*, vol. 60, pp. 457–476, 2020, doi: 10.1146/annurev-pharmtox-010919-023603.
[33] K. Ondrejkova, K. Sleiman, C. Veltkamp, F. Wang, G. Schneider, and D. Saur, "1657P Understanding the role of SAGA and mediator in the resistance to Pdk1 deletion in PDAC," *Annals of Oncology*, vol. 34, S913, 2023, doi: 10.1016/j.annonc.2023.09.2606.
[34] B. S. Atanassov *et al.,* "ATXN7L3 and ENY2 Coordinate Activity of Multiple H2B Deubiquitinases Important for Cellular Proliferation and Tumor Growth," (in eng), *Molecular cell*, vol. 62, no. 4, pp. 558–571, 2016, doi: 10.1016/j.molcel.2016.03.030.
[35] C. G. Gonzalez, S. Akula, and M. Burleson, "The role of mediator subunit 12 in tumorigenesis and cancer therapeutics," (in eng), *Oncology letters*, vol. 23, no. 3, p. 74, 2022, doi: 10.3892/ol.2022.13194.
[36] S. Anders and W. Huber, "Differential expression analysis for sequence count data," (in eng), *Genome biology*, vol. 11, no. 10, R106, 2010, doi: 10.1186/gb-2010-11-10-r106.
[37] K. R. Kukurba and S. B. Montgomery, "RNA Sequencing and Analysis," (in eng), *Cold Spring Harbor protocols*, vol. 2015, no. 11, pp. 951–969, 2015, doi: 10.1101/pdb.top084970.
[38] A. Liberzon, C. Birger, H. Thorvaldsdóttir, M. Ghandi, J. P. Mesirov, and P. Tamayo, "The Molecular Signatures Database (MSigDB) hallmark gene set collection," (in eng), *Cell systems*, vol. 1, no. 6, pp. 417–425, 2015, doi: 10.1016/j.cels.2015.12.004.
[39] V. Tamási, K. Monostory, R. A. Prough, and A. Falus, "Role of xenobiotic metabolism in cancer: involvement of transcriptional and miRNA regulation of P450s," (in eng), *Cellular and molecular life sciences : CMLS*, vol. 68, no. 7, pp. 1131–1146, 2011, doi: 10.1007/s00018-010-0600-7.
[40] W. Chen, Z. Zhang, S. Zhang, P. Zhu, J. K.-S. Ko, and K. K.-L. Yung, "MUC1: Structure, Function, and Clinic Application in Epithelial Cancers," (in eng), *International journal of molecular sciences*, vol. 22, no. 12, 2021, doi: 10.3390/ijms22126567.
[41] J. Yu *et al.,* "Oncogenic Role of NUPR1 in Ovarian Cancer," (in eng), *OncoTargets and therapy*, vol. 13, pp. 12289–12300, 2020, doi: 10.2147/OTT.S262224.
[42] M. C. Mendoza, E. E. Er, and J. Blenis, "The Ras-ERK and PI3K-mTOR pathways: cross-talk and compensation," (in eng), *Trends in biochemical sciences*, vol. 36, no. 6, pp. 320–328, 2011, doi: 10.1016/j.tibs.2011.03.006.
[43] M. Roliński *et al.,* "Loss of Mediator complex subunit 13 (MED13) promotes resistance to alkylation through cyclin D1 upregulation," (in eng), *Nucleic acids research*, vol. 49, no. 3, pp. 1470–1484, 2021, doi: 10.1093/nar/gkaa1289.